

# Decay constants with Wilson fermions at $\beta = 6.0$

Tanmoy Bhattacharya and Rajan Gupta

*T-8, MS-B285, Los Alamos National Laboratory, Los Alamos, NM 87545*

We present results of a high statistics study of  $f_\pi$ ,  $f_K$ ,  $f_D$ ,  $f_{D_s}$ , and  $f_V^{-1}$  in the quenched approximation using Wilson fermions at  $\beta = 6.0$  on  $32^3 \times 64$  lattices. We find that the various sources of systematic errors (due to setting the quark masses, renormalization constant, and lattice scale) are now larger than the statistical errors. Our best estimates, without extrapolation to the continuum limit, are  $f_\pi = 134(4)$  MeV,  $f_K = 159(3)$  MeV,  $f_D = 229(7)$  MeV,  $f_{D_s} = 260(4)$  MeV, and  $f_V^{-1}(m_\rho) = 0.33(1)$ , where only statistical errors have been shown. We discuss the extrapolation to the continuum limit by combining our data with those from other collaborations.

## 1. Introduction

Phenomenologically,  $f_D$ ,  $f_{D_s}$ ,  $f_B$  and  $f_{B_s}$  are essential ingredients needed to determine the less well known elements of the Cabibbo-Kobayashi-Maskawa mixing matrix. As these heavy-light decay constants are at best very poorly measured, there has been a large effort by many lattice groups to estimate them from numerical simulations. Decay constants are amongst the most precise quantities that one can calculate on the lattice and a recent review has been presented by Allton at LATTICE95 [1]. In this paper we present results for  $f_\pi$ ,  $f_K$ ,  $f_K/f_\pi$ ,  $f_D$ ,  $f_D/f_\pi$ ,  $f_{D_s}$ ,  $f_{D_s}/f_D$ , and vector decay constant  $f_V^{-1}$  from simulations done on  $170\ 32^3 \times 64$  quenched lattices at  $\beta = 6.0$  using Wilson fermions. We emphasize that extrapolations to the continuum limit, incorporating the results from other collaborations, are not very reliable as the combined data do not show an unambiguous pattern of  $O(a)$  corrections.

Preliminary results from a subset of 100 lattices were presented at the LATTICE94 meeting [2]. The raw lattice results have not changed significantly since then, however we now present a more detailed analysis of the systematic errors. We estimate the uncertainty in the results due to extrapolation of the lattice data to physical values of the quark masses, the renormalization constants for the lattice currents, and the extraction of the lattice scale. We find that these various systematic errors are now much larger than the statistical errors. Finite size errors, if present, are smaller than the statistical errors. Our best estimates are now given in the scheme called *TAD1* to evaluate the renormalization constants for the axial and vector currents.

The details of the lattices and the calculation of the spectrum are given in a companion paper [3]. In section 2 we briefly summarize the lattice parameters, and in section 3 we describe the lattice methodology and the consistency checks made to extract the decay constants using estimates from different types of fits and interpolating operators. The choice of renormalization constants for the axial and vector currents,  $Z_A$  and  $Z_V$ , is discussed in section 4, the lattice scale in section 5, and the quark masses in section 6. In section 7 we compare the data with predictions of quenched chiral perturbation theory. The extrapolation of the data to physical values of quark masses is discussed in section 8, and our best estimates at  $\beta = 6.0$  are summarized in section 9. In section 10 we compare our data with those from other collaborations (GF11 [4], JLQCD [5], and APE [6]. The MILC data presented in [7] are preliminary and therefore not included in this analysis.) and extrapolate the combined data to the continuum limit. Finally, we present our conclusions in section 11.

## 2. LATTICE PARAMETERS

The details of the  $170\ 32^3 \times 64$  gauge lattices used in this analysis are given in [3]. We refer the interested reader to it for further details of the signal in the 2-point correlation functions and on the extraction of the spectrum. In this paper we concentrate on the analysis of systematic errors in decay constants associated with fixing the quark masses  $\overline{m} = (m_u + m_d)/2$ ,  $m_s$  and  $m_c$ , the renormalization constants  $Z_A$  and  $Z_V$ , and the extrapolation to physical masses and the continuum limit.

To calculate decay constants we used the Wuppertal source quark propagators at five values of quark mass given by  $\kappa = 0.135$  ( $C$ ),  $0.153$  ( $S$ ),  $0.155$  ( $U_1$ ),  $0.1558$  ( $U_2$ ), and  $0.1563$  ( $U_3$ ). These quarks correspond to pseudoscalar mesons of mass 2835, 983, 690, 545 and 431 MeV respectively where we have used  $1/a = 2.33$  GeV for the lattice scale. We construct two types of correlation functions, smeared-local ( $\Gamma_{SL}$ ) and smeared-smeared ( $\Gamma_{SS}$ ) which are combined in different ways to extract the decay constants as discussed below. The three light quarks allow us to extrapolate the data to the physical isospin symmetric light quark mass  $\bar{m}$ , while the  $C$  and  $S$   $\kappa$  values are selected to be close to the physical charm and strange quark masses. The physical value of strange quark lies between  $S$  and  $U_1$  and we use these two points to interpolate to it. In most cases we find that extrapolation to  $\bar{m}$  can be done using the six combinations of light quarks  $U_1U_1$ ,  $U_1U_2$ ,  $U_1U_3$ ,  $U_2U_2$ ,  $U_2U_3$ ,  $U_3U_3$ . For brevity we will denote this combination by  $\{U_iU_j\}$  and the three degenerate cases by  $\{U_iU_i\}$ .

### 3. Lattice Method for calculating $f_{PS}$ and $f_V$

The lattice definition of the pseudo-scalar decay constant  $f_{PS}$ , using the convention that the experimental value is  $f_\pi = 131$  MeV, is [8]

$$f_\pi = \frac{Z_A \langle 0 | A_4^{\text{local}} | \pi(\vec{p}) \rangle}{E_\pi(\vec{p})}, \quad (3.1)$$

where  $Z_A$  is the axial current renormalization constant connecting the lattice scheme to continuum  $\overline{MS}$ . In order to extract  $f_\pi$  we study, in addition to the 2-point correlation functions  $\Gamma$ , two kinds of ratios of correlators:

$$\begin{aligned} R_1(t) &= \frac{\Gamma_{SL}(t)}{\Gamma_{SS}(t)} \quad t \xrightarrow{\sim} \infty \quad \frac{\langle 0 | A_4^{\text{local}} | \pi \rangle}{\langle 0 | A_4^{\text{smeared}} | \pi \rangle} \\ R_2(t) &= \frac{\Gamma_{SL}(t)\Gamma_{SL}(t)}{\Gamma_{SS}(t)} \quad t \xrightarrow{\sim} \infty \quad \frac{|\langle 0 | A_4^{\text{local}} | \pi \rangle|^2}{2M_\pi} e^{-M_\pi t}. \end{aligned} \quad (3.2)$$

In the case of  $R_1$  we have to extract  $\langle 0 | A_4^{\text{smeared}} | \pi \rangle$  separately from the  $\Gamma_{SS}$  correlator. For each of the two ratios,  $R_1$  and  $R_2$ , the smeared source  $J$  used to create the pion can be either  $\pi$  or  $A_4$ . This gives four ways of calculating  $f_\pi$ , which we label as  $f_\pi^a$  (using ratio  $R_1$  with  $J = \pi$ ),  $f_\pi^b$  (using ratio  $R_1$  with  $J = A_4$ ),  $f_\pi^c$  (using ratio  $R_2$  with  $J = \pi$ ), and  $f_\pi^d$  (using ratio  $R_2$  with  $J = A_4$ ). The fifth way,  $f_\pi^e$ , consists of combining the mass and amplitude of the 2-point correlation functions  $\langle A_4 P \rangle_{LS}$  and  $\langle PP \rangle_{SS}$ , and the sixth way,  $f_\pi^f$ , uses  $\langle A_4 A_4 \rangle_{LS}$  and  $\langle A_4 A_4 \rangle_{SS}$ .

The lattice results for mesons at  $\vec{p} = 0$  for the different combinations of quarks are given in Table 1 using the renormalization scheme  $Z_{TAD1}$  defined in Table 5. All Errors are estimated by a single elimination Jackknife procedure. The results from the six ways of combining the two correlators are mutually consistent. Since the different methods use the same correlators, the data are highly correlated; however, consistent results do indicate that fits have been made to the lowest state in each of these correlators and reassure us of the statistical quality of the data.

|             | $f_\pi^a$ | $f_\pi^b$ | $f_\pi^c$ | $f_\pi^d$ | $f_\pi^e$ | $f_\pi^f$ |
|-------------|-----------|-----------|-----------|-----------|-----------|-----------|
| <i>ChCh</i> | 0.198(2)  | 0.198(3)  | 0.197(2)  | 0.197(2)  | 0.197(3)  | 0.197(3)  |
| <i>ChSt</i> | 0.129(2)  | 0.129(2)  | 0.129(2)  | 0.128(2)  | 0.129(2)  | 0.128(2)  |
| <i>ChU1</i> | 0.115(2)  | 0.116(2)  | 0.116(2)  | 0.115(2)  | 0.116(2)  | 0.115(2)  |
| <i>ChU2</i> | 0.110(2)  | 0.110(3)  | 0.111(2)  | 0.110(2)  | 0.111(2)  | 0.110(2)  |
| <i>ChU3</i> | 0.107(3)  | 0.108(3)  | 0.109(2)  | 0.108(2)  | 0.109(2)  | 0.108(2)  |
| <i>StSt</i> | 0.093(1)  | 0.093(1)  | 0.093(1)  | 0.093(1)  | 0.094(2)  | 0.093(2)  |
| <i>StU1</i> | 0.084(1)  | 0.084(1)  | 0.085(1)  | 0.084(1)  | 0.085(2)  | 0.084(1)  |
| <i>StU2</i> | 0.081(1)  | 0.080(1)  | 0.081(1)  | 0.081(1)  | 0.081(2)  | 0.080(2)  |
| <i>StU3</i> | 0.078(1)  | 0.078(1)  | 0.079(1)  | 0.078(1)  | 0.078(2)  | 0.077(2)  |
| <i>U1U1</i> | 0.076(1)  | 0.076(1)  | 0.077(1)  | 0.076(1)  | 0.076(2)  | 0.076(2)  |
| <i>U1U2</i> | 0.073(1)  | 0.072(1)  | 0.073(1)  | 0.073(1)  | 0.073(2)  | 0.072(2)  |
| <i>U1U3</i> | 0.070(1)  | 0.070(1)  | 0.071(1)  | 0.071(1)  | 0.070(2)  | 0.070(2)  |
| <i>U2U2</i> | 0.069(1)  | 0.069(1)  | 0.070(1)  | 0.069(1)  | 0.069(2)  | 0.069(2)  |
| <i>U2U3</i> | 0.067(1)  | 0.066(1)  | 0.068(1)  | 0.067(1)  | 0.066(2)  | 0.066(2)  |
| <i>U3U3</i> | 0.064(1)  | 0.064(1)  | 0.066(1)  | 0.065(1)  | 0.064(3)  | 0.064(2)  |

Table 1. The data, in lattice units, for the pseudo-scalar decay constant  $f_{PS}$  for the six different ways of combining the *SL* and *SS* correlators described in the text. The renormalization scheme used to generate this data is *TAD1* as described in Table 5, and the meson mass used in the analysis is taken to be the pole mass.

The results for  $f_\pi$  using correlators at non-zero momentum are given in Table 2. The data show that in almost all cases the results are consistent within  $2\sigma$ . The most noticeable differences are in the  $\vec{p} = (2, 0, 0)$  values for lighter quarks. The signal in these channels is not very good and it is likely that in these cases there exists contamination from excited states over the range of time-slices to which fits have been made. We regard the overall consistency of the data as another successful check of the lattice methodology. Henceforth we shall restrict the analysis to  $\vec{p} = (0, 0, 0)$  case as it has the best signal.

The dimensionless vector decay constants are defined as

$$Z_V \langle 0 | V_\mu^{\text{local}} | V \rangle = \frac{\epsilon_\mu M_V^2}{f_V} \quad (3.3)$$

where  $V_\mu$  is the vector current and  $|V\rangle$  is the lowest  $1^-$  state with mass  $M_V$ . The experi-

|             | $(\vec{p} = (0, 0, 0))$ | $(\vec{p} = (1, 0, 0))$ | $(\vec{p} = (1, 1, 0))$ | $(\vec{p} = (1, 1, 1))$ | $(\vec{p} = (2, 0, 0))$ |
|-------------|-------------------------|-------------------------|-------------------------|-------------------------|-------------------------|
| <i>ChCh</i> | 0.198(2)                | 0.198(2)                | 0.203(2)                | 0.200(3)                | 0.201(3)                |
| <i>ChSt</i> | 0.129(2)                | 0.129(2)                | 0.131(2)                | 0.129(2)                | 0.129(2)                |
| <i>ChU1</i> | 0.116(2)                | 0.116(2)                | 0.118(2)                | 0.115(2)                | 0.115(2)                |
| <i>ChU2</i> | 0.111(2)                | 0.111(2)                | 0.112(2)                | 0.110(2)                | 0.110(3)                |
| <i>ChU3</i> | 0.108(2)                | 0.108(3)                | 0.110(3)                | 0.107(3)                | 0.108(3)                |
| <i>StSt</i> | 0.093(1)                | 0.094(1)                | 0.095(2)                | 0.096(2)                | 0.099(2)                |
| <i>StU1</i> | 0.084(1)                | 0.085(1)                | 0.086(2)                | 0.087(2)                | 0.090(2)                |
| <i>StU2</i> | 0.080(1)                | 0.081(2)                | 0.082(2)                | 0.083(2)                | 0.086(2)                |
| <i>StU3</i> | 0.078(1)                | 0.079(2)                | 0.080(3)                | 0.080(2)                | 0.083(2)                |
| <i>U1U1</i> | 0.076(1)                | 0.077(2)                | 0.078(2)                | 0.079(2)                | 0.083(3)                |
| <i>U1U2</i> | 0.073(1)                | 0.073(2)                | 0.074(2)                | 0.075(3)                | 0.080(3)                |
| <i>U1U3</i> | 0.070(1)                | 0.071(2)                | 0.072(2)                | 0.072(3)                | 0.078(4)                |
| <i>U2U2</i> | 0.069(1)                | 0.070(2)                | 0.071(2)                | 0.071(3)                | 0.077(4)                |
| <i>U2U3</i> | 0.067(1)                | 0.068(2)                | 0.069(3)                | 0.068(3)                | 0.075(5)                |
| <i>U3U3</i> | 0.064(1)                | 0.066(2)                | 0.067(3)                | 0.064(4)                | 0.074(5)                |

Table 2. *The data, in lattice units, for the pseudo-scalar decay constant  $f_{PS}$ , averaged over the six different ways of combining the SL and SS correlators, measured at different momenta. The renormalization scheme is TAD1 as described in Table 5, and the meson mass used in the analysis is taken to be the pole mass.*

mental quantities are related to  $f_V^{-1}$  by

$$\begin{aligned}
f_\rho^{-1} &= \frac{1}{\sqrt{2}} f_V^{-1}(M_\rho) &= 0.199(5), \\
f_\phi^{-1} &= -\frac{1}{3} f_V^{-1}(M_\phi) &= -0.078(1), \\
f_{J/\psi}^{-1} &= \frac{2}{3} f_V^{-1}(M_{J/\psi}) &= 0.087(3),
\end{aligned} \tag{3.4}$$

where the values are calculated using the rate  $\Gamma(V \rightarrow e^+e^-)$  given in the PDB94 [9]. We extract the relevant matrix element in the same two ways as described in Eq. (3.2) for  $f_{PS}$ . To study discretization errors we study three lattice transcriptions of the vector current

(local, extended, and conserved),

$$\begin{aligned}
V_\mu^L(x) &= \bar{\psi}(x)\gamma_\mu\psi(x), \\
V_\mu^E(x) &= \bar{\psi}(x)\gamma_\mu U_\mu(x)\psi(x + \hat{\mu}) + \bar{\psi}(x + \hat{\mu})\gamma_\mu U_\mu^\dagger(x)\psi(x), \\
V_\mu^C(x) &= \bar{\psi}(x)(\gamma_\mu - r)U_\mu(x)\psi(x + \hat{\mu}) + \bar{\psi}(x + \hat{\mu})(\gamma_\mu + r) U_\mu^\dagger(x)\psi(x).
\end{aligned}
\tag{3.5}$$

where for degenerate quarks the last form is the conserved current. In Tables 3 and 4 we show the lattice data for the 15 mass combinations as a function of the different methods/currents, and versus the renormalization schemes for the local current. Overall, the data show that the two methods in Eq. (3.2) give consistent results for all three currents. The results from the local and extended vector currents also agree, while those from the conserved current are  $\approx 10\%$  smaller. These points will be discussed in more detail later.

In order to extract results that can be compared with experiments we analyze the data in terms of the five sources of systematic errors discussed below.

#### 4. The renormalization constant $Z_A$ and $Z_V$

Reliable calculations of decay constants depend on our ability to calculate the renormalization constants,  $Z_A$  and  $Z_V$ , linking the lattice and continuum regularization schemes. In our analysis we use 1-loop matching with the tadpole subtraction scheme of Lepage-Mackenzie. An outline of the scheme, which includes picking a good definition of the lattice  $\alpha_s$  and the scale  $q^*$  at which to evaluate it is as follows. Lepage and Mackenzie show that  $\alpha_v$  (to be defined below) is a better expansion parameter than the bare lattice coupling. To pick the value of  $q^*$  we need to know the “mean” momentum flow relevant to a given matrix element. Again it has been pointed out by Lepage and Mackenzie that  $q^*$ , estimated by calculating the mean momentum in the loop integrals, is dominated by tadpole diagrams which are lattice artifacts. If the tadpoles are not removed then this scale is typically  $\pi/a$ . They have proposed a meanfield improved version of the lattice theory which removes the contribution of tadpoles. The effect of this is three-fold. One, it typically changes  $q^*$  to  $1/a$ , *i.e.* the matching scale becomes more infrared if the tadpole diagram is removed; second the renormalization of the quark field changes from  $\sqrt{2\kappa} \rightarrow \sqrt{8\kappa_c}\sqrt{1 - 3\kappa/4\kappa_c}$ ; and finally the perturbative expression for  $8\kappa_c$  is combined with the coefficient of  $\alpha_v$  in the one loop matching relations to remove the tadpole contribution.

To get  $\alpha_{\overline{MS}}(q^*)$  we use the following Lepage-Mackenzie scheme. The coupling  $\alpha_v$  is defined at scale  $q = 3.41/a$  to be

$$\alpha_v\left(\frac{3.41}{a}\right) (1 - (1.19 + 0.017n_f)\alpha_v) = -\frac{3}{4\pi}\ln\left(\frac{1}{3}\text{Tr}Plaq\right),
\tag{4.1}$$

which is related to  $\alpha_{\overline{MS}}$  at scale  $q = 3.41/a$  by

$$\frac{1}{\alpha_{\overline{MS}}} = \frac{1}{\alpha_v} + 0.822.
\tag{4.2}$$

|          | $f_\rho^a \text{ Loc.}$ | $f_\rho^b \text{ Loc.}$ | $f_\rho^a \text{ Ext.}$ | $f_\rho^b \text{ Ext.}$ | $f_\rho^a \text{ Con.}$ | $f_\rho^b \text{ Con.}$ |
|----------|-------------------------|-------------------------|-------------------------|-------------------------|-------------------------|-------------------------|
| $ChCh$   | 0.186(02)               | 0.186(03)               | 0.184(03)               | 0.185(02)               | 0.168(03)               | 0.169(02)               |
| $ChSt$   | 0.184(03)               | 0.186(03)               | 0.190(04)               | 0.191(03)               | 0.171(03)               | 0.172(03)               |
| $ChU_1$  | 0.174(03)               | 0.176(03)               | 0.182(04)               | 0.182(03)               | 0.162(04)               | 0.164(03)               |
| $ChU_2$  | 0.170(04)               | 0.172(04)               | 0.177(05)               | 0.178(04)               | 0.157(05)               | 0.159(03)               |
| $ChU_3$  | 0.166(04)               | 0.170(05)               | 0.175(07)               | 0.176(05)               | 0.154(06)               | 0.157(04)               |
| $StSt$   | 0.291(04)               | 0.293(05)               | 0.303(06)               | 0.308(05)               | 0.268(05)               | 0.274(04)               |
| $StU_1$  | 0.300(04)               | 0.301(06)               | 0.312(07)               | 0.318(06)               | 0.273(06)               | 0.282(04)               |
| $StU_2$  | 0.302(04)               | 0.299(09)               | 0.314(08)               | 0.319(06)               | 0.273(07)               | 0.282(05)               |
| $StU_3$  | 0.303(05)               | 0.297(10)               | 0.313(11)               | 0.318(08)               | 0.271(09)               | 0.281(06)               |
| $U_1U_1$ | 0.316(05)               | 0.314(05)               | 0.329(10)               | 0.334(05)               | 0.285(09)               | 0.296(04)               |
| $U_1U_2$ | 0.320(05)               | 0.317(06)               | 0.334(13)               | 0.338(06)               | 0.288(11)               | 0.299(05)               |
| $U_1U_3$ | 0.322(06)               | 0.317(06)               | 0.333(16)               | 0.334(09)               | 0.288(14)               | 0.300(05)               |
| $U_2U_2$ | 0.325(06)               | 0.320(07)               | 0.338(17)               | 0.337(10)               | 0.292(15)               | 0.303(06)               |
| $U_2U_3$ | 0.326(07)               | 0.319(08)               | 0.334(23)               | 0.334(13)               | 0.292(20)               | 0.303(07)               |
| $U_3U_3$ | 0.326(07)               | 0.316(10)               | 0.326(31)               | 0.327(16)               | 0.291(27)               | 0.302(08)               |

Table 3. Lattice data for the vector decay constant  $f_V^{-1}$  for the two different ways of combining the  $SL$  and  $SS$  correlators, and for the three different lattice vector currents described in the text. The renormalization scheme in all cases is  $TAD1$  as described in Table 5, and the meson mass used in the analysis is taken to be the pole mass.

We then run  $\alpha_{\overline{MS}}$  from  $q$  to  $q^*$  by integrating the 2-loop  $\beta$ -function. To translate the results from  $q^*$  to any other point one uses the standard continuum running.

At the lowest order there are two equally good tadpole factors,  $U_0 = \text{plaquette}^{1/4}$  or  $8\kappa_c$ . To the accuracy of the meanfield improvement one expects  $8\kappa_c U_0 = 1$ . Deviations from this relation ( $\approx 10\%$  for the Wilson action at  $\beta = 6.0$ ) are a measure of possible residual errors. Writing the tadpole factor as  $1 - X\alpha_{\overline{MS}}(q^*)$ , we define a given  $Z$  factor to be

$$Z = 1 + \alpha_{\overline{MS}}(q^*) \left( \frac{\gamma_0}{4\pi} \log(q^* a) + (C - X) \right) \quad (4.3)$$

|          | $Z_{TADa}$ | $Z_{TAD1}$ | $Z_{TAD2}$ | $Z_{TAD\pi}$ | $Z_{TADU_0}$ | $Z_{Tfg11}$ | $Z_{BST\pi}$ |
|----------|------------|------------|------------|--------------|--------------|-------------|--------------|
| $ChCh$   | 0.184(2)   | 0.186(2)   | 0.193(2)   | 0.196(3)     | 0.173(2)     | 0.188(2)    | 0.119(2)     |
| $ChSt$   | 0.183(3)   | 0.185(3)   | 0.192(3)   | 0.195(3)     | 0.172(3)     | 0.187(3)    | 0.144(2)     |
| $ChU_1$  | 0.173(3)   | 0.175(3)   | 0.182(3)   | 0.185(3)     | 0.163(3)     | 0.177(3)    | 0.140(2)     |
| $ChU_2$  | 0.169(4)   | 0.171(4)   | 0.177(4)   | 0.180(4)     | 0.158(3)     | 0.172(4)    | 0.138(3)     |
| $ChU_3$  | 0.166(4)   | 0.168(5)   | 0.174(5)   | 0.177(5)     | 0.156(4)     | 0.169(5)    | 0.136(4)     |
| $StSt$   | 0.289(4)   | 0.292(4)   | 0.303(4)   | 0.308(4)     | 0.271(4)     | 0.295(4)    | 0.278(4)     |
| $StU_1$  | 0.297(5)   | 0.301(5)   | 0.312(5)   | 0.317(5)     | 0.279(4)     | 0.304(5)    | 0.294(5)     |
| $StU_2$  | 0.298(6)   | 0.301(6)   | 0.312(6)   | 0.317(6)     | 0.280(6)     | 0.304(6)    | 0.297(6)     |
| $StU_3$  | 0.297(7)   | 0.300(7)   | 0.311(7)   | 0.317(7)     | 0.279(6)     | 0.303(7)    | 0.298(7)     |
| $U_1U_1$ | 0.312(5)   | 0.315(5)   | 0.327(5)   | 0.333(5)     | 0.293(4)     | 0.318(5)    | 0.316(5)     |
| $U_1U_2$ | 0.315(5)   | 0.319(5)   | 0.331(5)   | 0.336(5)     | 0.296(5)     | 0.322(5)    | 0.322(5)     |
| $U_1U_3$ | 0.316(6)   | 0.319(6)   | 0.331(6)   | 0.337(6)     | 0.297(5)     | 0.322(6)    | 0.325(6)     |
| $U_2U_2$ | 0.319(6)   | 0.322(6)   | 0.335(6)   | 0.340(6)     | 0.300(6)     | 0.325(6)    | 0.329(6)     |
| $U_2U_3$ | 0.319(7)   | 0.322(7)   | 0.335(7)   | 0.340(7)     | 0.299(6)     | 0.325(7)    | 0.331(7)     |
| $U_3U_3$ | 0.318(8)   | 0.321(8)   | 0.334(8)   | 0.339(8)     | 0.299(7)     | 0.324(8)    | 0.332(8)     |

Table 4. Lattice data for the vector decay constant  $f_V^{-1}$  as a function of the different renormalization schemes given in Table 5. The results are for the local current, and the meson mass used in the analysis is taken to be the pole mass.

where  $C$  is the difference between the finite part of the continuum  $\overline{MS}$  and lattice 1-loop result. Thus,  $Z_A$  for the local operator in the tadpole improved schemes is

$$\sqrt{Z_\psi^1 Z_\psi^2 Z_A^L} = \sqrt{1 - 3\kappa_1/4\kappa_c} \sqrt{1 - 3\kappa_2/4\kappa_c} (1 - \alpha_{\overline{MS}}(q^*)(1.68 - X)). \quad (4.4)$$

In order to examine the dependence of the decay constants on  $Z$  and the renormalization of the quark field we present our results for seven different commonly used schemes described in Table 5. The schemes  $Z_{TADa}$ ,  $Z_{TAD1}$ ,  $Z_{TAD2}$ ,  $Z_{TAD\pi}$ , and  $Z_{Tfg11}$  are all self-consistent to  $O(\alpha_s)$ . The scheme  $Z_{TADU_0}$  is ad hoc as we have replaced  $8\kappa_c$  by  $U_0$  in only one part. We shall quote, as our best estimates, results obtained in the  $Z_{TAD1}$  scheme and use the difference between it and  $Z_{TAD\pi}$  as an estimate of the systematic error due



to tuning  $q^*$ . Finally, an estimate of the residual perturbative errors is taken to be the difference between  $Z_{TAD1}$  and  $Z_{TADU_0}$ , and is given in column labeled  $Z_A$  in Table 10. This, we believe, is an over-estimate of the error we make by using the 1-loop coefficient of  $\alpha_v$ .

|                 | $Z_{TADa}$                      | $Z_{TAD1}$                      | $Z_{TAD2}$                      | $Z_{TAD\pi}$                    | $Z_{TADU_0}$                    | $Z_{Tgf11}$                     | $Z_{Boost\pi}$ |
|-----------------|---------------------------------|---------------------------------|---------------------------------|---------------------------------|---------------------------------|---------------------------------|----------------|
| $Z_\psi$        | $1 - \frac{3\kappa}{4\kappa_c}$ | $1 - \frac{3\kappa}{4\kappa_c}$ | $1 - \frac{3\kappa}{4\kappa_c}$ | $1 - \frac{3\kappa}{4\kappa_c}$ | $1 - \frac{3\kappa}{4\kappa_c}$ | $1 - \frac{3\kappa}{4\kappa_c}$ | $2\kappa$      |
| Tadpole         | $1/8\kappa_c$                   | $1/8\kappa_c$                   | $1/8\kappa_c$                   | $1/8\kappa_c$                   | $U_0$                           | $1/8\kappa_c$                   | NO             |
| $q^*$           | $2 \text{ GeV}$                 | $1/a$                           | $2/a$                           | $\pi/a$                         | $1/a$                           | $1/a$                           | $\pi/a$        |
| $\alpha_s(q^*)$ | 0.202                           | 0.190                           | 0.151                           | 0.133                           | 0.190                           | 0.181                           | 0.133          |

Table 5. *The different renormalization schemes used in the analysis. The two possible tadpole factors are  $U_0 = plaq^{1/4} = 0.878$  and  $1/8\kappa_c = 0.795$ . The 1-loop perturbative expansions for these are  $U_0 = 1 - 1.0492\alpha$  and  $8\kappa_c = 1 + 1.364\alpha$  respectively. The sixth scheme  $Z_{Tgf11}$  is the one used by the GF11 collaboration with a slightly different definition of  $\alpha_{\overline{MS}}[4]$ .*

The renormalization of the local vector current,  $Z_V^L$  proceeds in the same way as  $Z_A$ . In case of both the extended and conserved currents, there is no tadpole contribution in  $C$  as it cancels between the wave-function renormalization and the vertex correction. Consequently, we use the non-perturbative value for  $8\kappa_c$ . The complete renormalization factors in the tadpole improved schemes for relating the lattice results to the continuum are

$$\begin{aligned}
\sqrt{Z_\psi^1 Z_\psi^2} Z_V^L &= \sqrt{1 - 3\kappa_1/4\kappa_c} \sqrt{1 - 3\kappa_2/4\kappa_c} (1 - \alpha_{\overline{MS}}(q^*)(2.182 - X)), \\
\sqrt{Z_\psi^1 Z_\psi^2} Z_V^E &= 8\kappa_c \sqrt{1 - 3\kappa_1/4\kappa_c} \sqrt{1 - 3\kappa_2/4\kappa_c} (1 - 1.038\alpha_{\overline{MS}}(q^*)), \\
\sqrt{Z_\psi^1 Z_\psi^2} Z_V^C &= 8\kappa_c \sqrt{1 - 3\kappa_1/4\kappa_c} \sqrt{1 - 3\kappa_2/4\kappa_c}.
\end{aligned} \tag{4.5}$$

We find that the results with the local current lie in between those from the extended and conserved currents, and have the best statistical signal. We therefore quote results from the local current as our best estimate, and use the difference between them as an estimate of the systematic error.

## 5. The lattice scale $a$

To convert lattice results to physical units we use the lattice scale extracted by setting  $M_\rho$  to its physical value. This gives  $1/a = 2.330(41) \text{ GeV}$  [3]. The variation of  $1/a$  between

the Jackknife samples is folded into our error analysis, however different ways of setting the scale are not. For example, using  $M_N$  to set the scale gives  $1/a = 2.018(37)$  GeV [3], while NRQCD simulations of the charmonium and  $\Upsilon$  spectrum give  $1/a = 2.4(1)$  GeV [10]. As we show later, the scale determined from  $f_\pi$  is 2265(57) MeV. Thus, estimates based on mesonic quantities like  $M_\rho$ , heavy-heavy spectrum, and  $f_\pi$  all give consistent results. We take  $1/a(M_\rho) = 2.330(41)$  GeV and use the spread,  $\sim 70$  MeV  $\sim 3\%$ , as our best guess of the size of scaling violations relevant to the analysis of the decay constants. To reduce this error requires using an improved gauge and fermion action, which is beyond the scope of this work.

## 6. Setting the quark masses

In order to extrapolate the lattice data to physical values of the quark mass we have to fix  $\bar{m}$ ,  $m_s$  and  $m_c$ . The chiral limit is determined by linearly extrapolating the data for  $M_\pi^2$  to zero using the six cases  $\{U_i U_j\}$ . Our best estimate is

$$\kappa_c = 0.157131(9), \quad (6.1)$$

which is used in the calculation of  $Z_\psi$ .

To fix the value of  $\kappa_l$  corresponding to  $\bar{m}$  we extrapolate the ratio  $M_\pi^2/M_\rho^2$  to its physical value 0.03182. The result is

$$\kappa_l = 0.157046(9) \quad (6.2)$$

Thus, our data is able to resolve between the chiral limit and  $\bar{m}$ . In [3] we had shown that a non-perturbative estimate of quark mass  $m_{np}$ , calculated using the Ward identity, and  $(1/2\kappa - 1/2\kappa_c)$  are linearly related for light quarks, so either definition of the quark mass can be used for the extrapolation. We have chosen to use  $m_{np}$  in this paper.

The determination of the strange quark mass has significant systematic errors as shown below. We determine  $\kappa_s$  in three ways as described in [3]. We extrapolate  $M_K^2/M_\pi^2$ ,  $M_{K^*}/M_\rho$ , and  $M_\phi/M_\rho$  to  $\bar{m}$  and then interpolate in the strange quark to match their physical value. In Table 6 we give  $\kappa_s$ , the non-perturbative estimate  $m_{np}a = m_s a$ , and  $m_s = Z_m(1/2\kappa - 1/2\kappa_c)$  evaluated at 2 GeV in the  $\overline{MS}$  scheme using the *TAD1* matching between lattice and continuum. The data show a  $\sim 20\%$  difference between various estimates of  $m_s$  which cannot be explained away as due to statistical errors. Using  $M_K^2/M_\pi^2$  to fix  $m_s$  implies that  $m_s \equiv 25\bar{m}$  as we use the lowest order chiral expansion to fit  $M_{PS}^2$  data. On the other hand  $M_\phi/M_\rho$  gives  $m_s/\bar{m} \approx 30$ . This estimate is not constrained by the chiral expansion, and is in surprisingly good agreement with the next-to-leading chiral result [11]. In this paper we shall quote results for both  $m_s(M_K)$  and  $m_s(M_\phi)$ , and take the values with  $m_s(M_\phi)$  as our best estimates. The difference in results between using  $m_s(M_K)$  and  $m_s(M_\phi)$  will be taken as an estimate of the systematic error due to the uncertainty in setting  $m_s$ .

|                  | $\kappa_s$  | $m_{s,np}a$ | $m_s$ (2 GeV) MeV |
|------------------|-------------|-------------|-------------------|
| $M_K^2/M_\rho^2$ | 0.15503(7)  | 0.0372(14)  | 129(2)            |
| $M_{K^*}/M_\rho$ | 0.15479(19) | 0.0421(36)  | 145(9)            |
| $M_\phi/M_\rho$  | 0.15464(17) | 0.0445(32)  | 154(8)            |

Table 6. Estimates of  $m_s$  using different combinations of hadron masses. We give the  $\kappa$  values, the quark mass determined by the Ward identity, and  $m_s = Z_m(1/2\kappa - 1/2\kappa_c)$  evaluated at 2 GeV in the  $\overline{MS}$  scheme, and using the TAD1 tadpole subtraction procedure.

To determine the value of  $\kappa$  corresponding to  $m_c$  we match  $M_D$ ,  $M_{D^*}$  and  $M_{D_s}$  as these are obtained from the same 2-point correlation functions as used to determine the decay constants. Unfortunately, as shown in [3], the estimate of charmonium and D meson masses measured from the rate of exponential fall-off of the 2-point function (pole mass or  $M_1$ ) and those from the kinetic mass defined as  $M_2 \equiv (\partial^2 E/\partial p^2|_{p=0})^{-1}$  are significantly different. We find that the data for the heavy-heavy and heavy-light  $q\bar{q}$  combinations are consistent with the nearest-neighbor symmetric-difference relativistic dispersion relation  $\sinh^2(E/2) - \sin^2(p/2) = \sinh^2(M/2)$ , in which case  $M_2$ , as defined above, is given by  $\sinh M$ . The results for  $M_1$  and  $M_2$  for the  $D$  states are given in Table 7 for  $\kappa = 0.135$  (we have simulated only one heavy quark mass). The data show that the experimental results lie between  $M_1$  and  $M_2$  for each of the three states, and the difference between  $M_1$  and  $M_2$  is large and statistically significant. The size of this systematic error and the uncertainty in setting the scale  $1/a$ , makes it difficult to fix  $\kappa_{charm}$ . We simply assume that  $\kappa = 0.135$  corresponds to  $m_c$ , and quote final results using  $M_2$ . As an estimate of systematic errors associated with not tuning  $m_c$  we take the difference in results between using  $M_1$  and  $M_2$  since we do not have access to the rate of variation of decay constants in the vicinity of  $m_c$ .

## 7. Quenched approximation

In the last couple of years it has been pointed out by Sharpe and collaborators [12] and by Bernard and Golterman [13] that there exist extra chiral logs due to the  $\eta'$ , which is also a Goldstone boson in the quenched approximation. These make the chiral limit of quenched quantities sick. To analyze the effects of quenching Bernard and Golterman [13] have constructed the ratio

$$R \equiv \frac{f_{12}^2}{f_{11'}f_{22'}} \quad (7.1)$$

applicable in a 4-flavor theory where  $m_1 = m_{1'}$  and  $m_2 = m_{2'}$ . The advantage of this ratio in comparing full and quenched theories is that it is free of ambiguities due to the cutoff  $\Lambda$  in loop integrals, and  $O(p^4)$  terms in the chiral Lagrangian. The chiral expression for  $R$

|                          | $M_1$    | $M_2$    | <i>Expt.</i> |
|--------------------------|----------|----------|--------------|
| $M_D$                    | 1805(31) | 1990(34) | 1869         |
| $M_{D^*}$                | 1876(32) | 2085(35) | 2008         |
| $M_{D_s}(m_s(M_K))$      | 1896(30) | 2112(32) | 1969         |
| $M_{D_s}(m_s(M_\phi))$   | 1914(26) | 2137(27) | 1969         |
| $M_{D_s^*}(m_s(M_K))$    | 1961(31) | 2201(34) | 2110?        |
| $M_{D_s^*}(m_s(M_\phi))$ | 1978(27) | 2224(29) | 2110?        |

Table 7. A comparison of lattice estimates of  $D$  meson masses with the experimental data. We show results for  $M_1$  and  $M_2$  and for the two different ways of setting  $m_s$  described in the text.

in the quenched theory is

$$R^Q = 1 + \delta \left[ \frac{m_{12}^2}{(m_{11'}^2 - m_{22'}^2)} \log \frac{m_{11'}^2}{m_{22'}^2} - 1 \right] + O((m_1 - m_2)^2), \quad (7.2)$$

where  $\delta \equiv m_0^2/24\pi^2 f_\pi^2$  parameterizes the effects of the  $\eta'$ . The analogous expression in full QCD is

$$R^F = 1 + \frac{1}{32\pi^2 f^2} \left[ m_{11'}^2 \text{Ln} \frac{m_{11'}^2}{m_{12}^2} + m_{22'}^2 \text{Ln} \frac{m_{22'}^2}{m_{12}^2} \right] + O((m_1 - m_2)^2). \quad (7.3)$$

The leading analytic corrections in both cases are  $O((m_1 - m_2)^2)$  [14], and were not included in the analysis presented at LATTICE 94 [15]. The data, shown in Figs. 1 and 2, indicates the need for including them in the fits. ( $X_{quenched}$  is the coefficient of  $\delta$  in Eq. (7.2), and  $X_{full}$  is the complete chiral logarithm term in Eq. (7.3).) The fit to the quenched expression, Fig. 1, gives  $\delta = 0.14(4)$ . The fit to full QCD expression has smaller  $\chi^2$  if we leave the intercept as a free parameter. In that case the fit gives 1.69(45) and not unity as required by Eq. (7.3). Thus, the effect of chiral logs is small, barely discernible from the statistical errors, and partly due to normal higher order terms in the chiral expansion. We shall therefore neglect the effects of quenched chiral logs in this study, and only discuss deviations of  $f_{PS}$  from a behavior linear in  $m_q$  at the appropriate places.

The second consequence of using the quenched approximation is that the coefficients in the chiral expansion are different in the quenched and full theories. This difference can be evaluated by comparing quenched and full QCD data, which is beyond the scope of this work. Thus, we cannot provide any realistic estimates of errors due to using the quenched approximation.

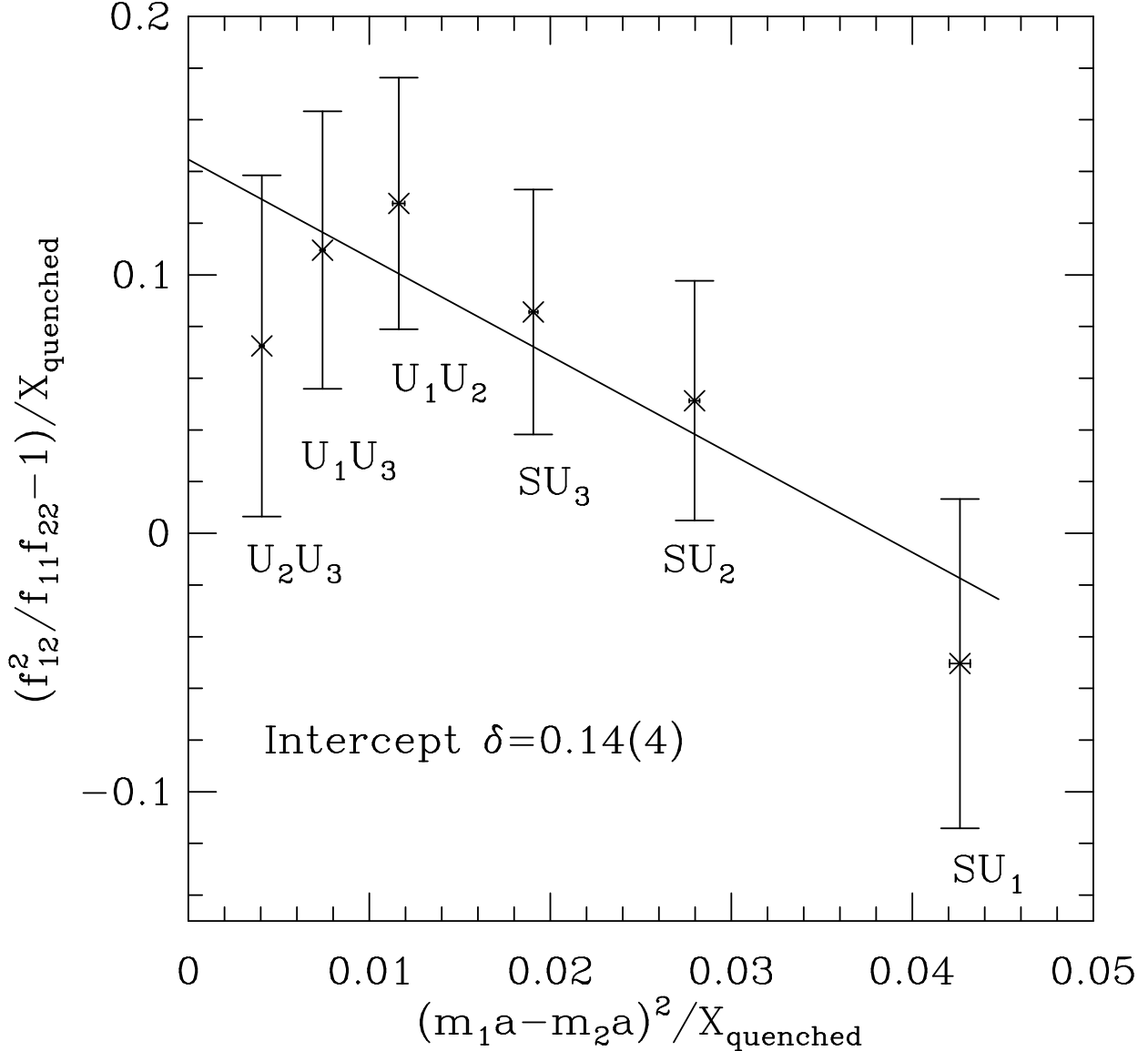


**Fig. 1:** Bernard-Golterman ratio  $R$  versus  $(m_1 - m_2)^2$ .  $X_{\text{quenched}}$  is the coefficient of  $\delta$  defined in Eq. (7.2). The intercept gives  $\delta = 0.14(4)$ .

## 8. Extrapolation in quark masses

In Fig. 3 we show the pseudoscalar data for  $\{U_i U_j\}$  and  $\{SS, SU_i\}$  combinations along with two different linear fits, one to the six  $\{U_i U_j\}$  data points ( $f_{PSa} = 0.0572(14) + 0.51(2)ma$ ) and the other to the four  $SS$  and  $\{SU_i\}$  points ( $f_{PSa} = 0.0568(14) + 0.48(1)ma$ ). Here  $m$  is the average mass of the quark and anti-quark. The data show that even though the slopes for the two fits are different, the values after extrapolation are virtually indistinguishable. The size of the break between the  $\{SS, SU_i\}$  and  $\{U_i U_j\}$  cases at  $m_s$  is right at the  $1\sigma$  level, and no such break is visible between the  $U_1 U_i$  and the  $U_2 U_2$  cases. We thus extrapolate to  $f_\pi$  using  $\{U_i U_j\}$  points and assume that

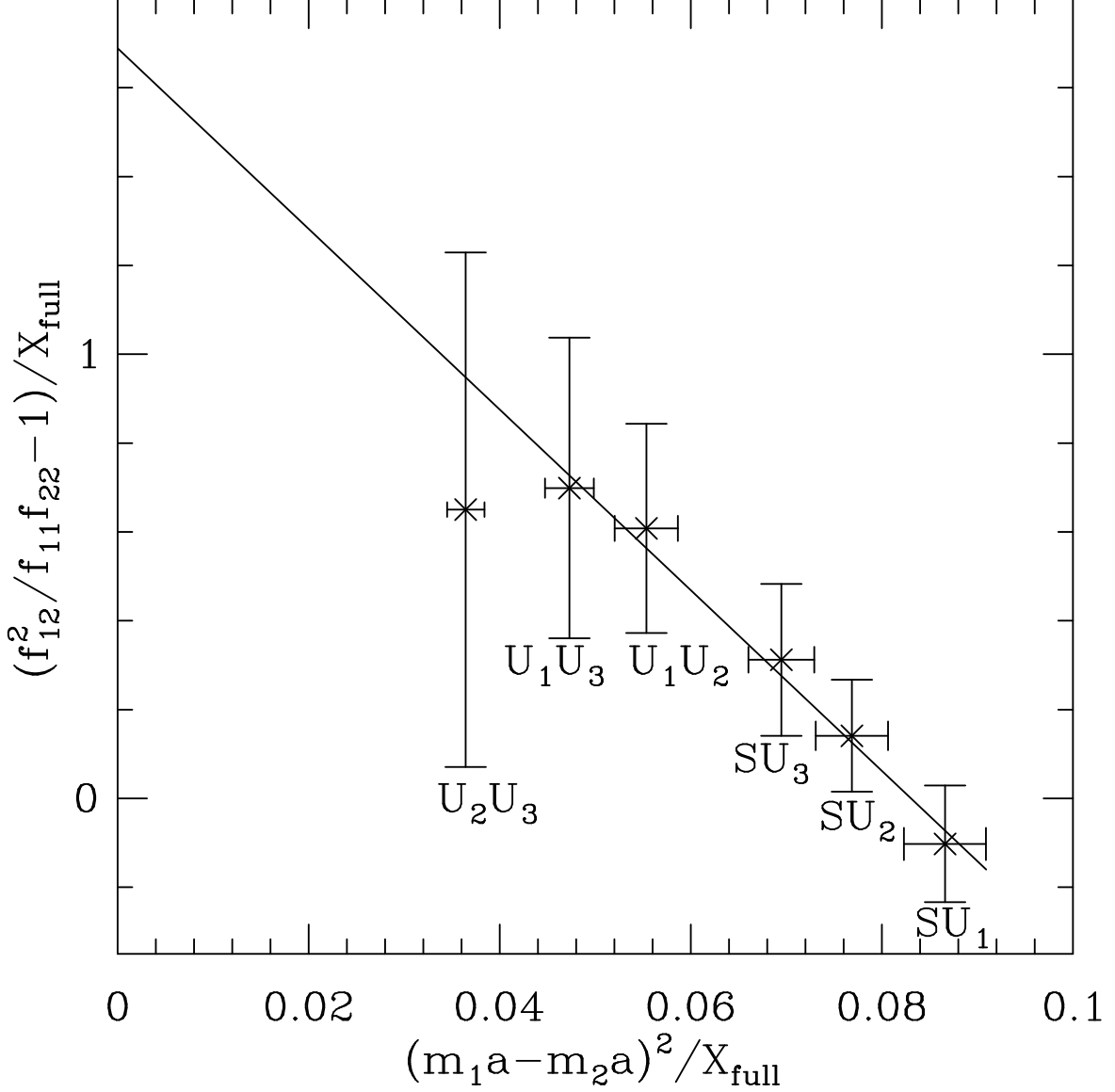


**Fig. 2:** Bernard-Golterman ratio  $R$  versus  $(m_1 - m_2)^2$ .  $X_{full}$  is the chiral correction defined in Eq. (7.2). The linear fit gives an intercept of 1.69(45) instead of unity as indicated by Eq. (7.3).

the overall jackknife error adequately includes the uncertainty due to extrapolation.

In Fig. 4 we show the extrapolation for heavy-light mesons for three cases of “heavy” ( $C$ ,  $S$ ,  $U_1$ ) quarks. The linear fits in the light quark mass,

$$\begin{aligned}
 f_{PS}a &= 0.103(3) + 0.33(5)m_{np}a & (CU_i), \\
 f_{PS}a &= 0.074(1) + 0.26(1)m_{np}a & (SU_i), \\
 f_{PS}a &= 0.067(1) + 0.25(1)m_{np}a & (U_1U_i),
 \end{aligned} \tag{8.1}$$

fit the data extremely well in each of the three cases. Deviations from linearity are apparent

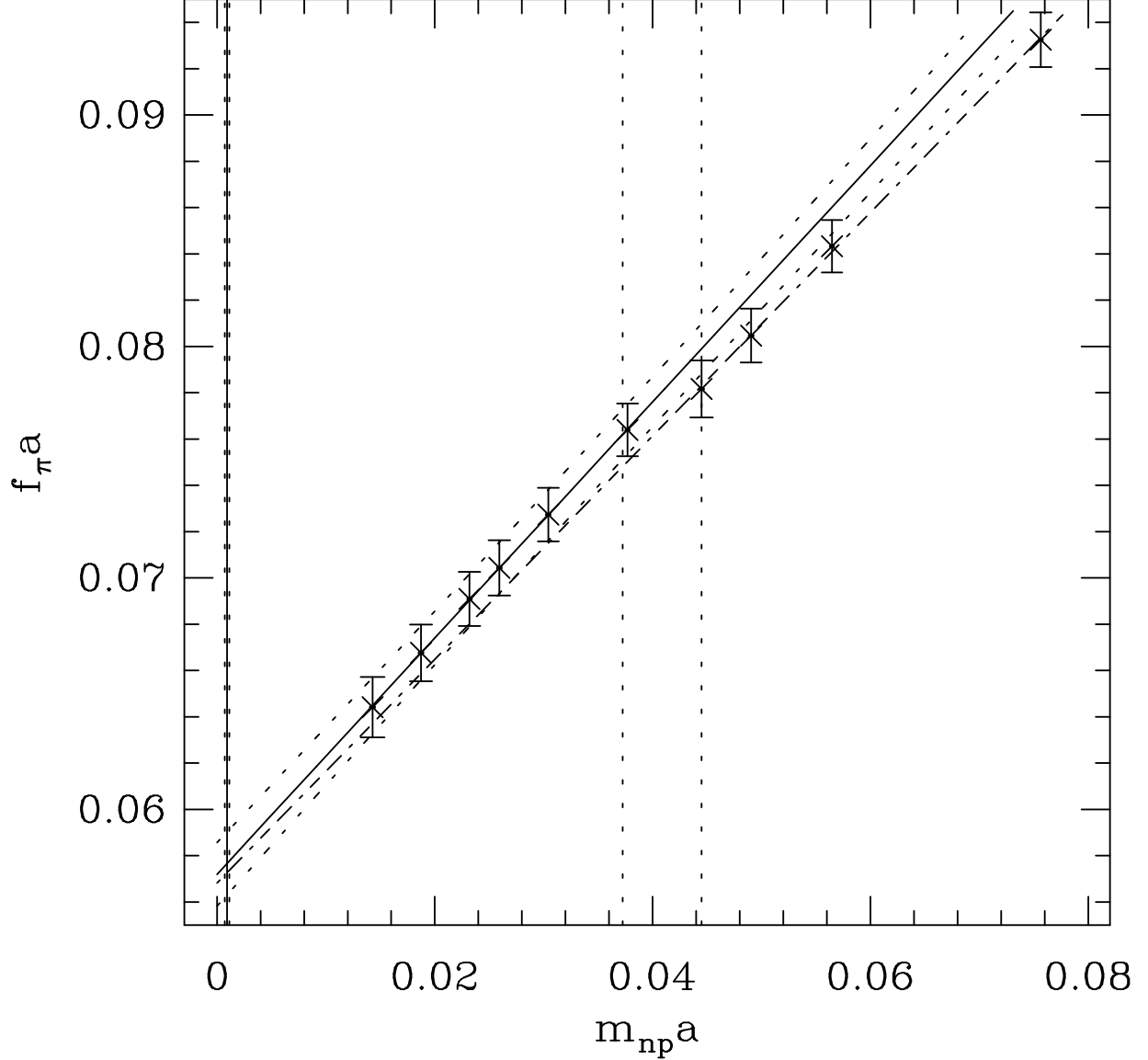


**Fig. 3:** Plot of data for  $f_\pi a$  versus  $m_{np}a$ . The linear fit, shown as a solid line, is to the six  $\{U_i U_j\}$  points. The error estimate on the fit is shown by the dotted lines. The dash-dot line is a linear fit to the four  $SS$  and  $\{SU_i\}$  points. The vertical line at  $m_{np}a \approx 0$  represents  $\bar{m}$  and the band at  $m_{np}a \approx 0.04$  denotes the range of  $m_s$ .

if the “light” quark mass is taken to be  $S$  as shown by the fourth point at  $m_{np}a = 0.076$ . These can be taken into account by including corrections, *i.e.* chiral logs and/or a quadratic term. A fit including a quadratic term fits all four points exceedingly well, however the extrapolated value changes by  $< 0.2\sigma$  in all three cases. Also, the change in curvature between  $U_1 U_i$  and  $CU_i$  is within the error estimates. Considering that the form of the correction term is not unique, and that the linear and quadratic fits give essentially the

same result, we consider it sufficient to use a linear fit to the three  $U_i$  points to extrapolate the heavy-light decay constants to  $\bar{m}$ .

The difference in slope between fits to  $\{U_i U_j\}$  and  $\{SU_i\}$  points does effect the value of  $f_K$ . We, therefore, calculate it in two ways; the central value is taken by extrapolating the  $\{SU_i\}$  and  $\{U_1 U_i\}$  data in the light quark to  $\bar{m}$  and then interpolating in the “heavy” to  $m_s$ . In the second way we use the slope determined from  $\{U_i U_j\}$  points and extrapolate to  $\bar{m} + m_s$ . The two give consistent results and we use the difference as an estimate of the systematic error.

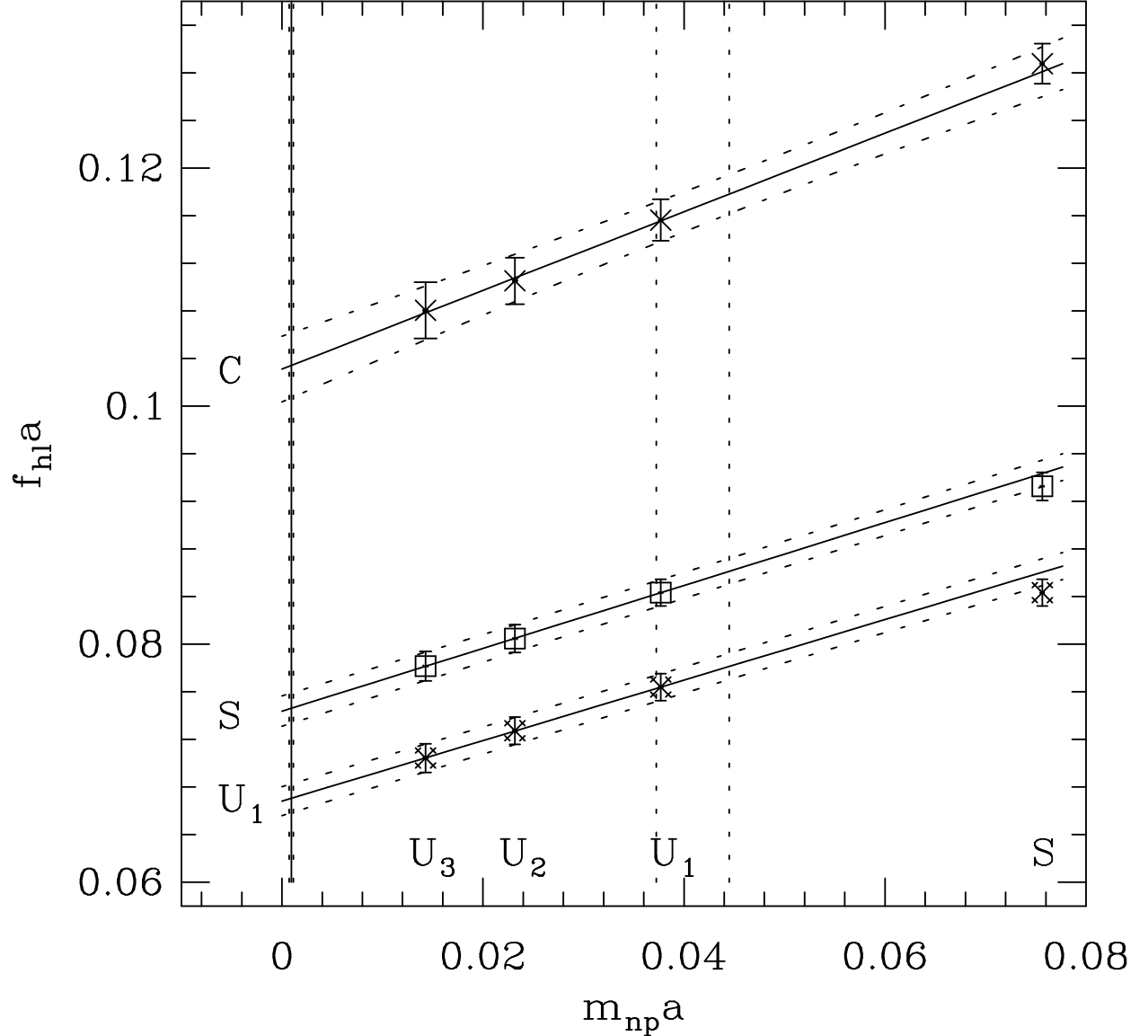


**Fig. 4:** Extrapolation of heavy-light pseudoscalar decay constants for three cases of “heavy”,  $C$ ,  $S$ ,  $U_1$  quarks. The linear fits are to the three “light”  $U_i$  quarks, and the fourth point (light quark is  $S$ ) is included to show the breakdown of the linear approximation.



The analogous plots for  $f_V^{-1}$  are shown in Figs. 5 and 6. To extract  $f_\rho^{-1}$  we make linear fits to the six  $\{U_i U_j\}$  and the three  $\{U_i U_i\}$  points. As shown in Fig. 5, these two fits are almost identical ( $f_V a = 0.328(10) + 0.33(23)m_{np}a$ ) and neither of them fits the data very well. The  $\{SU_i\}$  points show a very significant break from the  $\{U_i U_j\}$  points, so to extract  $f_{K^*}$ ,  $f_{D^*}$  we use the fits shown in Fig. 6. As in the case of  $f_{PS}$ , a linear fit to the three cases ( $CU_i, SU_i, U_1 U_i$ ) works well. The fit parameters are

$$\begin{aligned} f_V a &= 0.163(6) + 0.31(10) m_{np}a && (CU_i), \\ f_V a &= 0.300(9) + 0.026(14)m_{np}a && (SU_i), \\ f_V a &= 0.322(7) - 0.18(10) m_{np}a && (U_1 U_i), \end{aligned} \tag{8.2}$$

Note that the slope changes sign between the  $SU_i$  and  $U_1 U_i$  cases. Since the points at  $m_{np}a = 0.076$  ( $S$ ) show deviations from the linear fits, we do not include this point in our analysis.

## 9. Results at $\beta = 6.0$

The results for the pseudoscalar decay constants, in lattice units, are given in Table 8 for each of the seven renormalization schemes. The table also shows the variation with respect to the two choices of  $m_s$  and whether one uses  $M_1$  or  $M_2$  for the heavy-light meson mass. For our best estimates we use  $Z_{TAD1}$ , and convert this data to MeV using  $1/a(M_\rho)$ . The results are summarized in Table 9 where we again display variation with respect to  $m_s$  and the heavy-light meson mass.

Our final results are shown in Table 10 along with the estimates of the various systematic errors discussed above. Thus, at  $\beta = 6.0$  the value of  $f_\pi$  come out about 3% larger. Using  $f_\pi$  data to set the lattice scale gives  $1/a(f_\pi) = 2265(57)$  MeV, whereas  $1/a(M_\rho) = 2330(41)$  MeV [3]. Even ignoring the various systematic errors, the two estimates differ by roughly  $1\sigma$ .

The ratio  $f_K/f_\pi = 1.186(16)$  is about  $2\sigma$  smaller than the experimental value 1.223 if one ignores all systematic errors. (The systematic error in fixing  $m_s$  would tend to lower our estimate, *i.e.* further increasing the difference.) An under-estimate of this ratio in the quenched approximation is consistent with predictions of quenched CPT [12] [13].

The major uncertainty in the results for the heavy-light cases,  $f_D$  and  $f_{D_s}$ , comes from the uncertainty in  $Z_A$  and in setting the charm mass. These corrections can be significant, and we need to reduce the various sources of systematic errors in order to extract reliable continuum estimates.

In Tables 11 and 12 we give the values for the vector decay constant  $f_V^{-1}$ , extrapolated to the masses of a number of vector states even though some of them do not decay electromagnetically to  $l^+ l^-$ . These tables also give the variation with respect to setting  $m_s$ , the heavy-light meson mass ( $M_1$  or  $M_2$ ),  $q^*$ ,  $Z_A$ , and the dependence on the lattice current. The criteria that the three types of currents should give consistent results justifies using the Lepage-Mackenzie procedure for  $V_i^C$  also, as pointed out by Bernard in [16]. Using the  $\sqrt{2\kappa}$  normalization for  $V_i^C$  (*i.e.* the same normalization as  $V_4^C(p_\mu = 0)$  which is constrained by the value of the conserved charge) gives significantly smaller values for cases with  $C$  quarks.

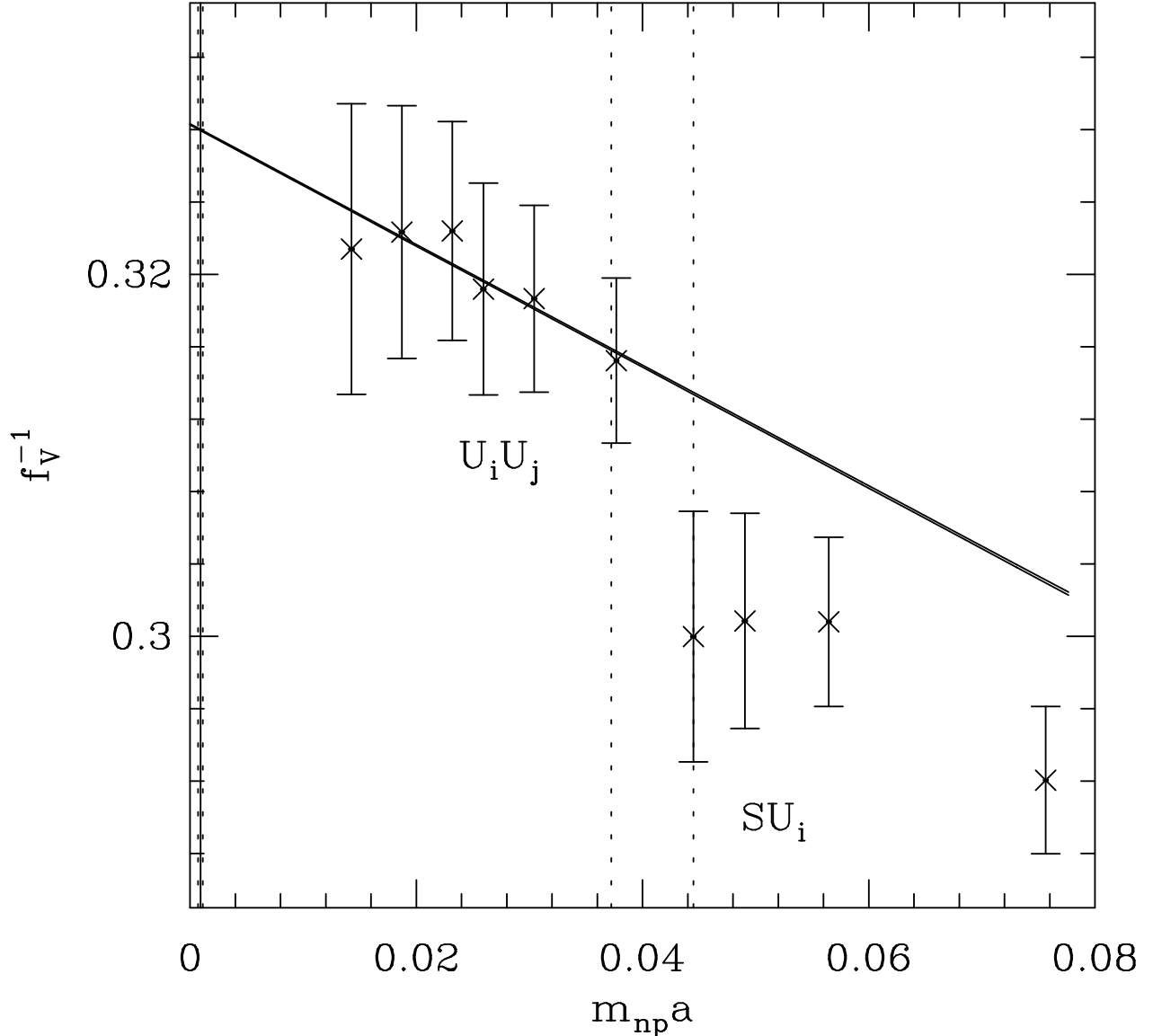


**Fig. 5:** Plot of data for  $f_V^{-1}$  versus  $m_{np}a$ . The linear fit is almost identical for the six  $\{U_i U_j\}$  or three  $\{U_i U_i\}$  points. The  $SS$  and  $\{SU_i\}$  points are also shown for comparison.

## 10. Infinite volume continuum results

In the companion paper analyzing the meson and baryon spectrum [3] we show that there are no noticeable differences between results obtained on  $24^3$  (earlier calculations) and our  $32^3$  lattices. Thus we do not apply any finite size corrections to our data. To extract results valid in the continuum limit we combine our data with those from the GF11 ( $\beta = 5.7, 5.93, 6.17$ ) [4], JLQCD ( $\beta = 6.1, 6.3$ ) [5], and APE ( $\beta = 6.0, 6.2$ ) [6] Collaborations. We have attempted to correct for as many systematic differences, however some like differences in lattice volumes, range of quark masses analyzed, and fitting techniques remain.

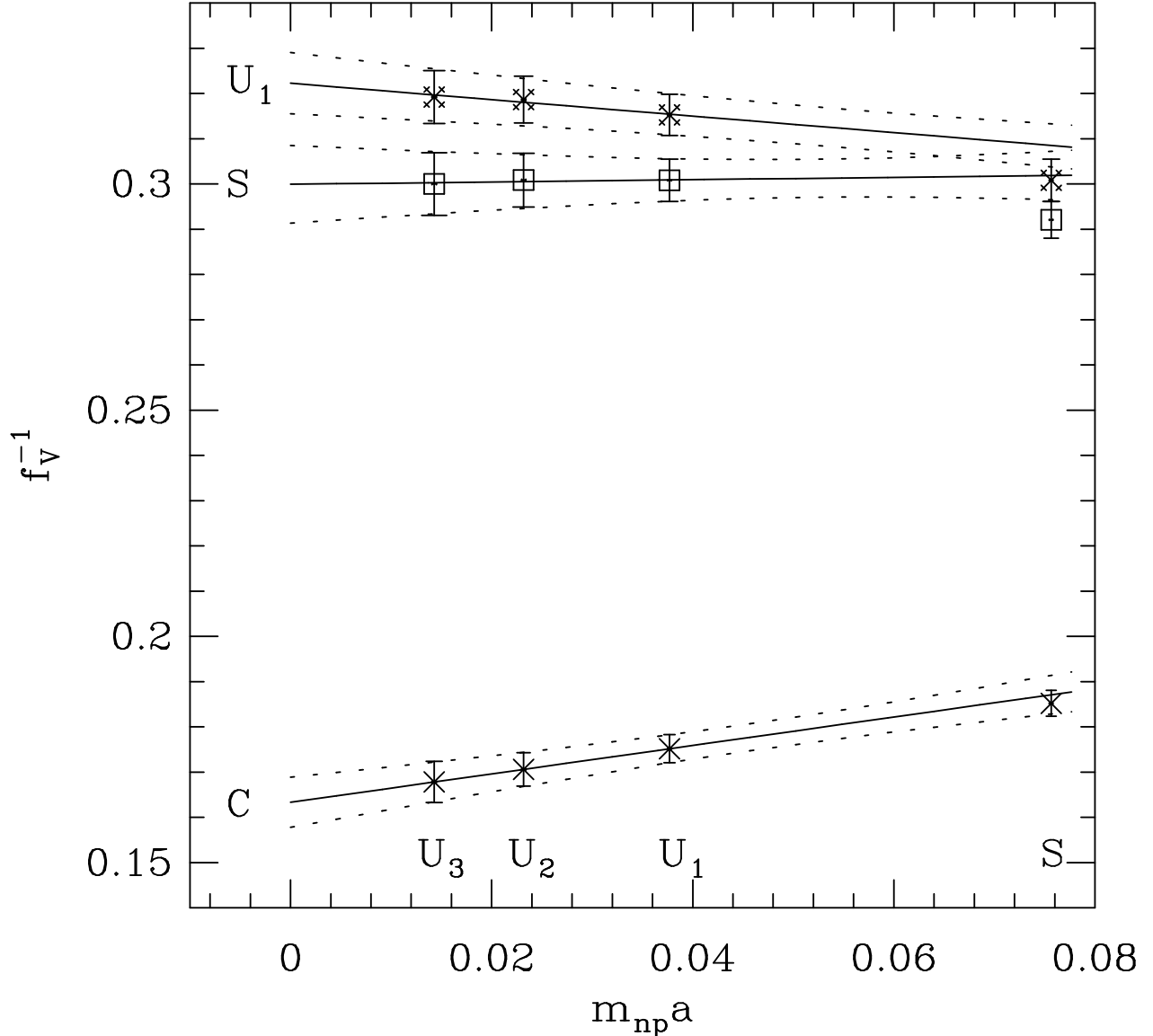


**Fig. 6:** *Extrapolation of heavy-light vector decay constants for three cases of “heavy”,  $C$ ,  $S$ ,  $U_1$  quarks. The linear fits are to the three “light”  $U_i$  quarks, and the fourth point (light quark is  $S$ ) is included to show the breakdown of the linear approximation.*

We first compare the data for  $f_\pi$  and  $f_K$  from the different collaborations as shown in Figs. 7 and 8. The various calculations have similar statistics (within a factor of two) and the two largest physical volumes used are by GF11 ( $24^3$  at  $\beta = 5.7$ ) and LANL ( $32^3$  at  $\beta = 6.0$ ) collaborations. To facilitate comparison we make three changes; (a) we switch to the convention in which  $f_\pi = 93$  MeV, (b) use the  $Z_{Tgf11}$  scheme, and (c) set  $m_s$  using  $M_K$ . A noticeable difference in the data shown in Figs. 7 and 8 is that the APE points at  $\beta = 6.0$  lie about  $1\sigma$  higher than LANL’s and the value of  $m_\rho a$  is also larger. We believe that the difference is partly a result of extrapolation from heavier quarks (APE

|                 |               | $Z_{TADa}$ | $Z_{TAD1}$ | $Z_{TAD2}$ | $Z_{TAD\pi}$ | $Z_{TADU_0}$ | $Z_{Tgf11}$ | $Z_{Boost\pi}$ |
|-----------------|---------------|------------|------------|------------|--------------|--------------|-------------|----------------|
| $(M_1)$         | $f_\pi$       | 0.057(01)  | 0.058(01)  | 0.058(01)  | 0.059(01)    | 0.054(01)    | 0.058(01)   | 0.060(01)      |
| $(M_1, M_K)$    | $f_K$         | 0.067(01)  | 0.067(01)  | 0.068(01)  | 0.068(01)    | 0.063(01)    | 0.067(01)   | 0.068(01)      |
| $(M_1, M_\phi)$ | $f_K$         | 0.068(01)  | 0.068(01)  | 0.069(01)  | 0.070(01)    | 0.064(01)    | 0.069(01)   | 0.069(01)      |
| $(M_1, M_K)$    | $f_K/f_\pi$   | 1.161(11)  | 1.161(11)  | 1.161(11)  | 1.161(11)    | 1.161(11)    | 1.161(11)   | 1.127(10)      |
| $(M_1, M_\phi)$ | $f_K/f_\pi$   | 1.186(16)  | 1.186(16)  | 1.186(16)  | 1.186(16)    | 1.186(16)    | 1.186(16)   | 1.145(14)      |
| $(M_1)$         | $f_D$         | 0.103(03)  | 0.103(03)  | 0.105(03)  | 0.105(03)    | 0.097(03)    | 0.104(03)   | 0.083(02)      |
| $(M_2)$         | $f_D$         | 0.098(02)  | 0.098(03)  | 0.100(03)  | 0.100(03)    | 0.092(02)    | 0.099(03)   | 0.079(02)      |
| $(M_1)$         | $f_D/f_\pi$   | 1.793(49)  | 1.793(49)  | 1.793(49)  | 1.793(49)    | 1.793(49)    | 1.793(49)   | 1.388(38)      |
| $(M_2)$         | $f_D/f_\pi$   | 1.705(45)  | 1.705(45)  | 1.705(45)  | 1.705(45)    | 1.705(45)    | 1.705(45)   | 1.320(35)      |
| $(M_1, M_K)$    | $f_{D_s}$     | 0.115(02)  | 0.115(02)  | 0.117(02)  | 0.118(02)    | 0.108(02)    | 0.116(02)   | 0.091(01)      |
| $(M_2, M_K)$    | $f_{D_s}$     | 0.109(02)  | 0.109(02)  | 0.111(02)  | 0.111(02)    | 0.102(02)    | 0.110(02)   | 0.086(01)      |
| $(M_1, M_\phi)$ | $f_{D_s}$     | 0.118(02)  | 0.118(02)  | 0.120(02)  | 0.120(02)    | 0.110(02)    | 0.118(02)   | 0.092(01)      |
| $(M_2, M_\phi)$ | $f_{D_s}$     | 0.111(02)  | 0.112(02)  | 0.113(02)  | 0.114(02)    | 0.104(02)    | 0.112(02)   | 0.087(01)      |
| $(M_1, M_K)$    | $f_{D_s}/f_D$ | 1.117(19)  | 1.117(19)  | 1.117(19)  | 1.117(19)    | 1.117(19)    | 1.117(19)   | 1.088(18)      |
| $(M_2, M_K)$    | $f_{D_s}/f_D$ | 1.112(18)  | 1.112(18)  | 1.112(18)  | 1.112(18)    | 1.112(18)    | 1.112(18)   | 1.083(17)      |
| $(M_1, M_\phi)$ | $f_{D_s}/f_D$ | 1.141(22)  | 1.141(22)  | 1.141(22)  | 1.141(22)    | 1.141(22)    | 1.141(22)   | 1.106(20)      |
| $(M_2, M_\phi)$ | $f_{D_s}/f_D$ | 1.135(21)  | 1.135(21)  | 1.135(21)  | 1.135(21)    | 1.135(21)    | 1.135(21)   | 1.100(19)      |

Table 8. Summary of results for pseudoscalar decay constants in lattice units. The variation with  $m_s$  (set by  $M_K$  or  $M_\phi$ ) and the heavy-light meson mass ( $M_1$  or  $M_2$ ) are shown explicitly. The Jackknife error estimates include statistical and a part of systematic errors due to extrapolation in quark masses.

collaboration use a linear fit to extrapolate data at  $\kappa = 0.153, 0.154, 0.155$  to the chiral limit). We find that both  $f_{PS}$  and  $M_V$  [3] data show negative curvature, and a linear extrapolation using only  $SS$  and  $U_1U_1$  points increases LANL estimates, accounting for the full difference in  $M_\rho$  and a part of that in  $f_\pi$ . The more important feature of the data, however is that neither plot shows a clear  $a$  dependence. Nevertheless, a linear fit to all

|           | $M_1 \ \& \ m_s(m_K)$ | $M_1 \ \& \ m_s(m_\phi)$ | $M_2 \ \& \ m_s(m_K)$ | $M_2 \ \& \ m_s(m_\phi)$ |
|-----------|-----------------------|--------------------------|-----------------------|--------------------------|
| $f_\pi$   | 134.4(41)             |                          |                       |                          |
| $f_K$     | 156.1(37)             | 159.4(33)                |                       |                          |
| $f_D$     | 241.0(75)             |                          | 229.2(70)             |                          |
| $f_{D_s}$ | 269.1(54)             | 275.0(46)                | 254.8(51)             | 260.1(44)                |

Table 9. Results for decay constants in the  $Z_{TAD1}$  scheme as a function of  $m_s$  and heavy-light meson masses. The data have been converted to MeV using  $M_\rho$  to set the scale. Only the jackknife error estimates are given.

|               | Best Estimate | Statistical & Extrapolation | Tuning $m_s$ | Tuning $m_c$ | $q^*$ | Tuning $a$ (3%) | $Z_A$ |
|---------------|---------------|-----------------------------|--------------|--------------|-------|-----------------|-------|
| $f_\pi$       | 134           | 4                           | –            | –            | +2    | 4               | 10    |
| $f_K$         | 159           | 3                           | –3           | –            | +3    | 5               | 10    |
| $f_D$         | 229           | 7                           | –            | +12          | +4    | 7               | 14    |
| $f_{D_s}$     | 260           | 4                           | –5           | +15          | +4    | 8               | 20    |
| $f_K/f_\pi$   | 1.19          | 0.02                        | –0.025       | –            | –     | –               | 0     |
| $f_D/f_\pi$   | 1.71          | 0.05                        | –            | +0.09        | –     | –               | ?     |
| $f_{D_s}/f_D$ | 1.135         | 0.021                       | –0.023       | +0.006       | –     | –               | 0     |

Table 10. Our final results using  $TAD1$  scheme along with estimates of statistical and various systematic errors as described in the text. All dimensionful numbers are given in MeV with the scale set by  $M_\rho$ . For the systematic errors due to  $m_s$ ,  $m_c$ ,  $q^*$  we also give the sign of the effect. We cannot estimate the uncertainty due to using the quenched approximation. Also, we do not have useful estimates for entries marked with a ?.

|                 |               | $Z_{TADa}$ | $Z_{TAD1}$ | $Z_{TAD2}$ | $Z_{TAD\pi}$ | $Z_{TAD8k}$ | $Z_{Tgf11}$ | $Z_{Boost\pi}$ |
|-----------------|---------------|------------|------------|------------|--------------|-------------|-------------|----------------|
| $(M_1)$         | $[M_\rho]$    | 0.324(10)  | 0.328(10)  | 0.340(11)  | 0.346(11)    | 0.305(09)   | 0.331(10)   | 0.345(11)      |
| $(M_1, M_K)$    | $[M_{K^*}]$   | 0.319(06)  | 0.322(06)  | 0.335(07)  | 0.340(07)    | 0.300(06)   | 0.325(06)   | 0.331(06)      |
| $(M_1, M_\phi)$ | $[M_{K^*}]$   | 0.315(06)  | 0.318(06)  | 0.330(06)  | 0.336(06)    | 0.296(06)   | 0.321(06)   | 0.325(06)      |
| $(M_1, M_K)$    | $[M_\phi]$    | 0.312(04)  | 0.316(04)  | 0.328(05)  | 0.333(05)    | 0.293(04)   | 0.318(04)   | 0.316(04)      |
| $(M_1, M_\phi)$ | $[M_\phi]$    | 0.308(04)  | 0.311(04)  | 0.323(05)  | 0.328(05)    | 0.289(04)   | 0.314(04)   | 0.309(05)      |
| $(M_1)$         | $[M_{D^*}]$   | 0.162(05)  | 0.164(05)  | 0.170(06)  | 0.173(06)    | 0.152(05)   | 0.165(06)   | 0.134(04)      |
| $(M_2)$         | $[M_{D^*}]$   | 0.137(04)  | 0.139(04)  | 0.144(04)  | 0.147(04)    | 0.129(04)   | 0.140(04)   | 0.114(03)      |
| $(M_1, M_K)$    | $[M_{D_s^*}]$ | 0.173(03)  | 0.175(03)  | 0.182(03)  | 0.185(03)    | 0.163(03)   | 0.177(03)   | 0.140(03)      |
| $(M_2, M_K)$    | $[M_{D_s^*}]$ | 0.145(02)  | 0.147(02)  | 0.152(03)  | 0.155(03)    | 0.136(02)   | 0.148(02)   | 0.117(02)      |
| $(M_1, M_\phi)$ | $[M_{D_s^*}]$ | 0.175(03)  | 0.177(03)  | 0.184(03)  | 0.187(03)    | 0.164(03)   | 0.179(03)   | 0.141(03)      |
| $(M_2, M_\phi)$ | $[M_{D_s^*}]$ | 0.146(02)  | 0.148(02)  | 0.154(03)  | 0.156(03)    | 0.138(02)   | 0.149(02)   | 0.118(02)      |

Table 11. Results for  $f_V^{-1}$  extrapolated to the masses of a number of vector states specified within [ ] as a function of the renormalization schemes,  $m_s$  ( $M_K$  or  $M_\phi$ ), and meson mass ( $M_1$  or  $M_2$ ).

data, assuming that lattice spacing errors are  $O(a)$ , gives

$$\begin{aligned} \frac{f_\pi}{M_\rho} &= 0.110(5) \quad (\text{expt. } 0.120), \\ \frac{f_K}{M_\rho} &= 0.121(4) \quad (\text{expt. } 0.147). \end{aligned} \tag{10.1}$$

with  $\chi^2/dof = 1.6$  and  $1.7$  respectively. The change from the GF11 results is marginal as the fit is still strongly influenced by the point at  $\beta = 5.7$ , which may lie outside the domain of validity of the linear extrapolation. A linear extrapolation excluding the  $\beta = 5.7$  data gives

$$\begin{aligned} \frac{f_\pi}{M_\rho} &= 0.118(10), \\ \frac{f_K}{M_\rho} &= 0.132(8), \end{aligned} \tag{10.2}$$

with  $\chi^2/dof = 2.1$  and  $1.9$  respectively. Using  $m_s(M_\phi)$  would increase  $f_K$  by  $\sim 2\%$ . Given the large difference in the extrapolated value depending on whether the data at  $\beta = 5.7$  is

|                 |               | <i>LOCAL</i> | <i>EXTENDED</i> | <i>CONSERVED</i> |
|-----------------|---------------|--------------|-----------------|------------------|
| $(M_1)$         | $[M_\rho]$    | 0.328(10)    | 0.335(26)       | 0.304(18)        |
| $(M_1, M_K)$    | $[M_{K^*}]$   | 0.322(06)    | 0.338(13)       | 0.297(10)        |
| $(M_1, M_\phi)$ | $[M_{K^*}]$   | 0.318(06)    | 0.334(12)       | 0.293(09)        |
| $(M_1, M_K)$    | $[M_\phi]$    | 0.316(04)    | 0.332(06)       | 0.291(06)        |
| $(M_1, M_\phi)$ | $[M_\phi]$    | 0.311(04)    | 0.327(06)       | 0.287(05)        |
| $(M_1)$         | $[M_{D^*}]$   | 0.164(05)    | 0.171(06)       | 0.151(05)        |
| $(M_2)$         | $[M_{D^*}]$   | 0.139(04)    | 0.146(05)       | 0.128(04)        |
| $(M_1, M_K)$    | $[M_{D_s^*}]$ | 0.175(03)    | 0.182(03)       | 0.163(03)        |
| $(M_2, M_K)$    | $[M_{D_s^*}]$ | 0.147(02)    | 0.152(03)       | 0.137(03)        |
| $(M_1, M_\phi)$ | $[M_{D_s^*}]$ | 0.177(03)    | 0.183(03)       | 0.164(03)        |
| $(M_2, M_\phi)$ | $[M_{D_s^*}]$ | 0.148(02)    | 0.153(03)       | 0.138(03)        |

Table 12. Results for  $f_V^{-1}$  as a function of the different discretizations of the vector current. We also show the dependence on  $m_s$  ( $M_K$  or  $M_\phi$ ) and meson mass ( $M_1$  or  $M_2$ ).

included or not makes it clear that more data are required to make a reliable extrapolation to the continuum limit.

The  $f_D$  and  $f_{D_s}$  data are combined with results from JLQCD [5] and APE [6] collaborations as shown in Fig. 9. The results are in  $TAD1$  scheme, and for comparison we use  $m_s(M_K)$ . Also, from here on we switch back to the convention in which  $f_\pi = 131$  MeV. The APE collaboration use  $M_1$  for the meson mass. For consistency we have shifted their data to  $M_2$  using our estimates given in Table 10. A linear extrapolation to  $a = 0$  then gives

$$\begin{aligned}
f_D &= 186(29) \text{ MeV}, \\
f_{D_s} &= 218(15) \text{ MeV},
\end{aligned}
\tag{10.3}$$

with  $\chi^2/dof = 2.2$  and  $2.0$  respectively. Using  $m_s(M_\phi)$  would increase  $f_{D_s}$  to  $224(16)$  MeV. The quality of the fits is, however, not very satisfactory. We feel that in order to improve the reliability of estimates in Eq. (10.3) one needs to reduce the various systematic errors that have not been included in the  $a \rightarrow 0$  extrapolations presented above.

Finally, a linear fit to  $f_\rho^{-1}$  data is shown in Fig. 10. The extrapolated value,  $0.16(2)$  with  $\chi^2/dof = 1.8$ , is smaller than the experimental value  $0.199(5)$ , and also smaller than

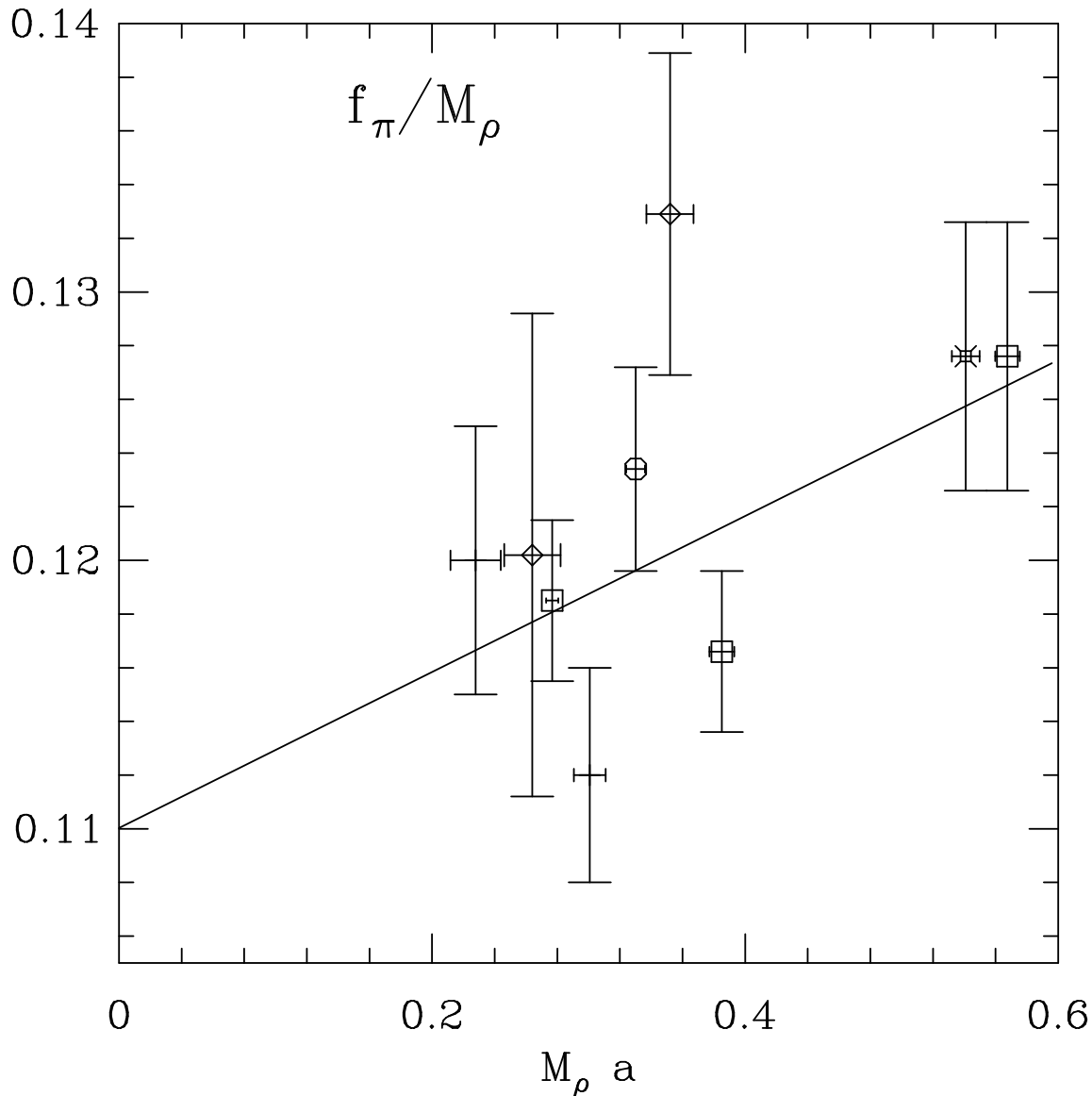


**Fig. 7:** Linear extrapolation to the continuum limit of the ratios  $f_\pi/M_\rho$ . Our data is shown with the symbol octagon, squares and fancy squares are the points from the GF11 Collaboration [4], diamonds are APE collaboration points [6], and the plus symbol labels JLQCD [5] data. The two GF11 points at  $M_\rho a \approx 0.56$  represent  $16^3$  (squares) and  $24^3$  (fancy squares) lattices at  $\beta = 5.7$ .

that from a fit to just the GF11 data which gives 0.18(2) [4].

## 11. Conclusions

We have presented a detailed analysis of the decay constants involving light-light and heavy-light (up to charm) quarks. We find that the various sources of systematic errors



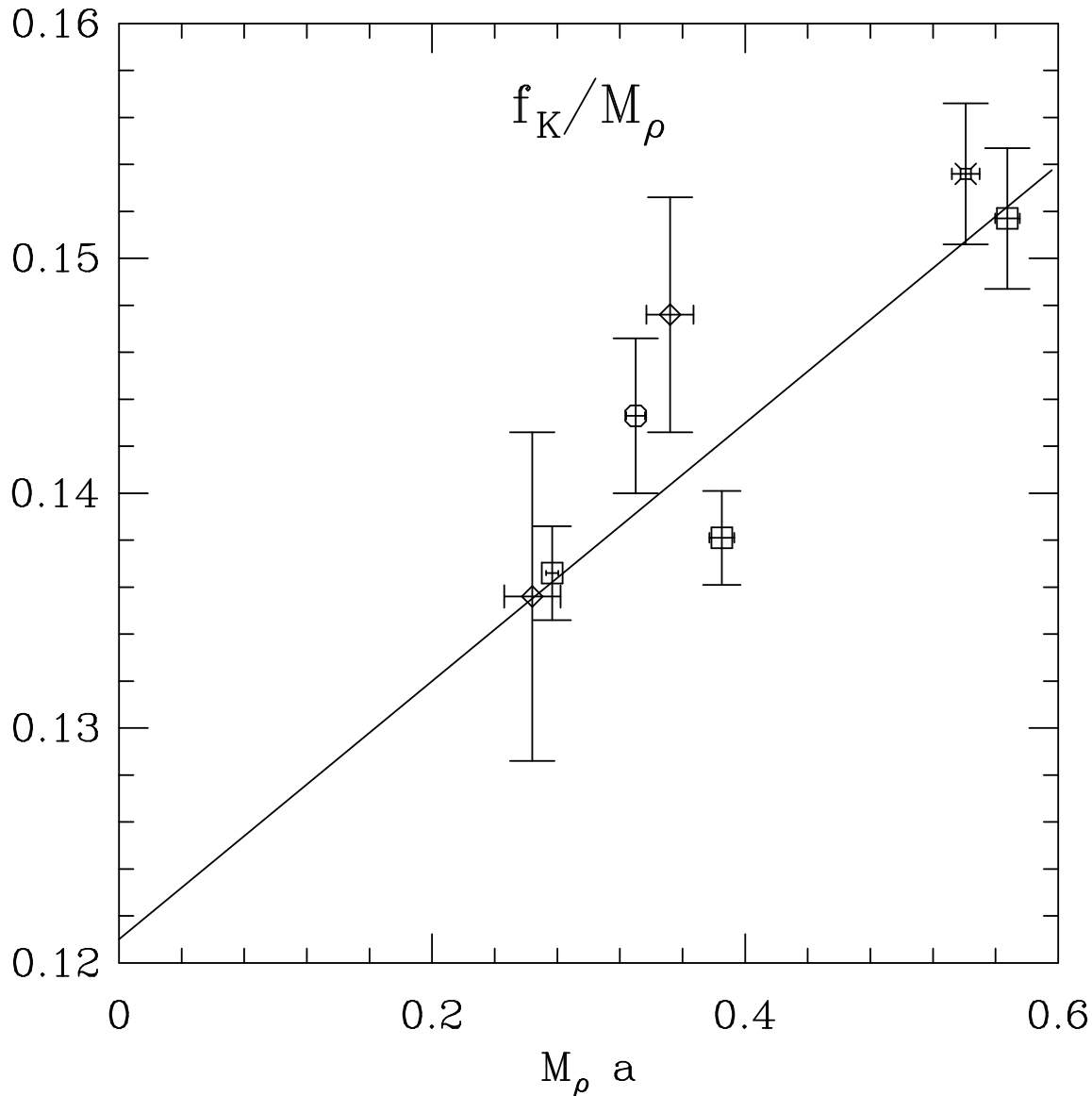


**Fig. 8:** *Linear extrapolation to the continuum limit of the ratios  $f_K/M_\rho$ . Our data is shown with the symbol octagon, the squares and fancy squares are the points from the GF11 Collaboration [4], and the diamond labels APE [6] data.*

(due to setting the quark masses, renormalization constant, and lattice scale) are now larger than the statistical errors. Work is under progress to address these issues. Our best estimates for the pseudo-scalar decay constants and the various sources of error, without extrapolation to the continuum limit, are given in Table 10.

We would like to stress that including all of the present high-statistics large lattice data, the extrapolation to the continuum limit is, in all cases, not very reliable. For the Wilson action the corrections are  $O(a)$ , and one expects that a linear extrapolation should suffice starting at some  $\beta$ . We find that in all cases the combined world data do not show

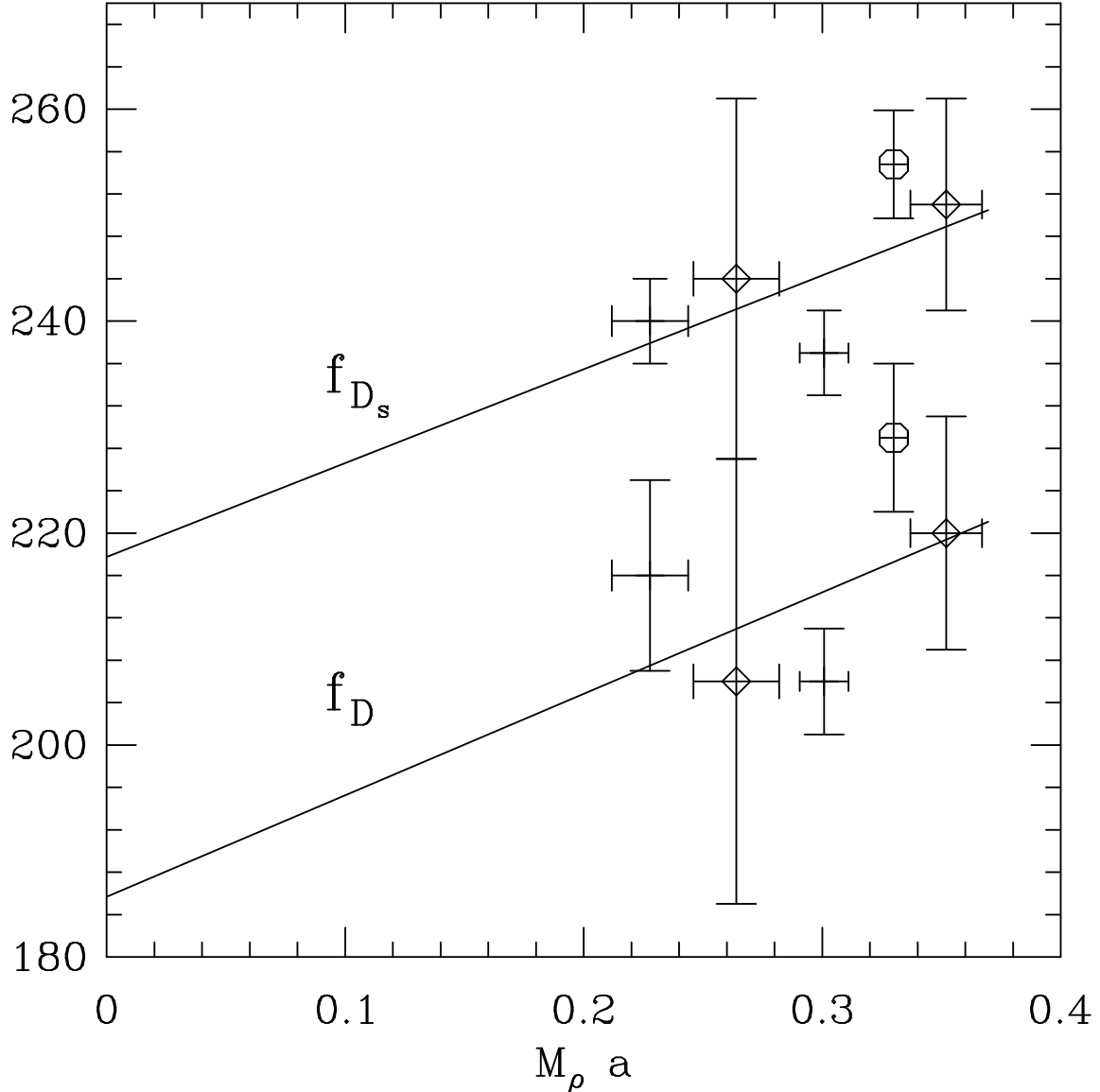


**Fig. 9:** *Extrapolation to the continuum limit of  $f_D$  and  $f_{D_s}$  (in MeV) data. Our data is shown with the symbol octagon, the plus points are from the JLQCD Collaboration [5], and the diamonds label the APE collaboration [6] data.*

an unambiguous linear behavior in  $a$ . Since different groups analyze the data in different ways, there is no clean way of including the systematic errors in individual points in the fits. We, therefore, cannot resolve whether the poor quality of the linear fits is due to the various systematic and statistical errors or due to the presence of higher order corrections. As a result, our overall conclusion is that precise data at a few more values of  $\beta$  are required in order to extract reliable results in the  $a \rightarrow 0$  limit.

We have made linear fits to the data with and without including the point at the strongest coupling,  $\beta = 5.7$ . A linear fit to combined world data gives  $f_\pi = 120(6)$  MeV

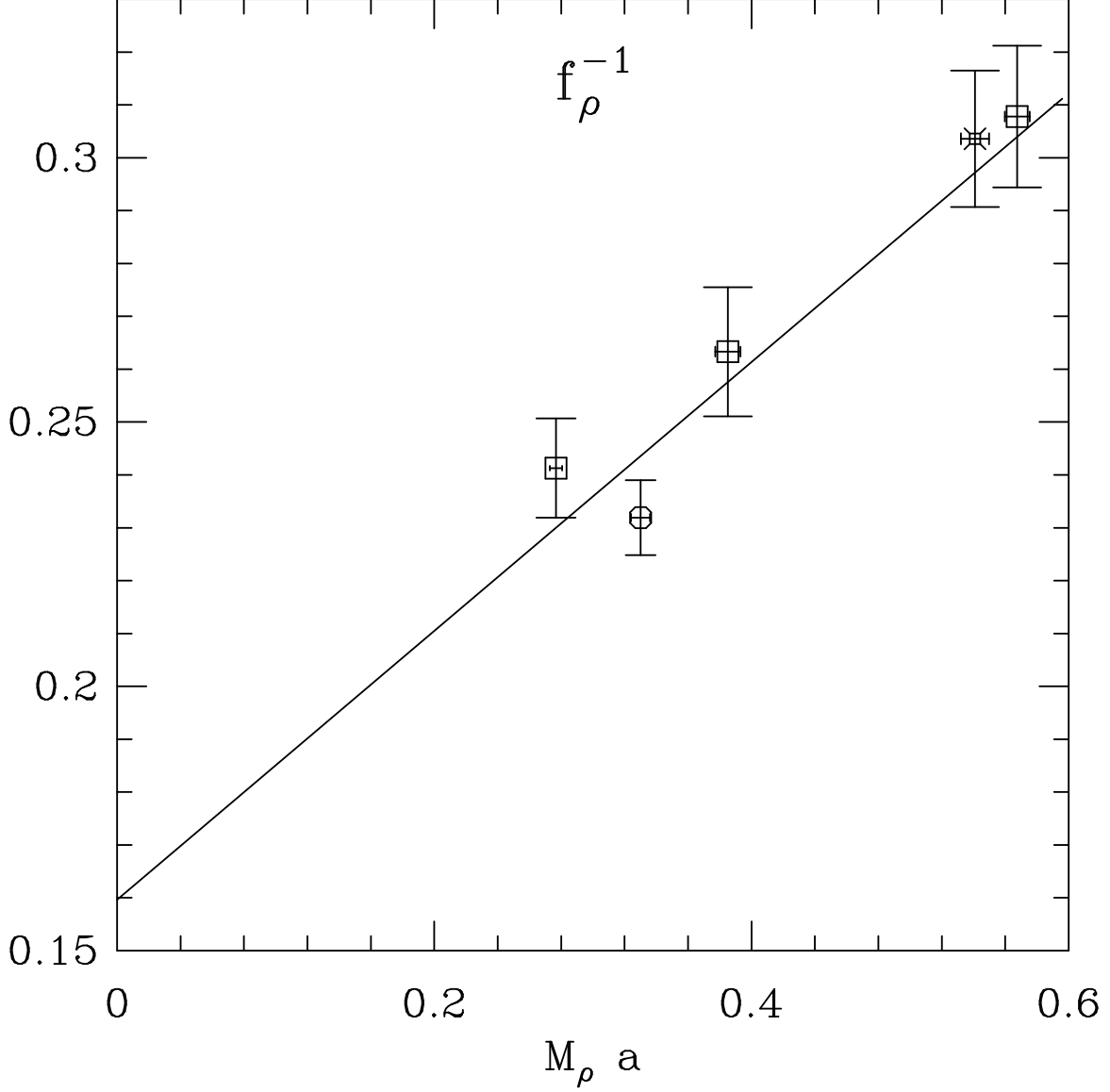


**Fig. 10:** *Extrapolation to the continuum limit of  $f_\rho^{-1}$ . Our data is shown with the symbol octagon, and the rest of the points are from the GF11 Collaboration [4].*

and  $f_K = 135(5)$  MeV. Excluding  $\beta = 5.7$  point changes these estimates to  $f_\pi = 128(6)$  and  $f_K = 146(5)$  MeV. Our best estimates for heavy-light meson,  $f_D = 186(29)$  MeV and  $f_{D_s} = 218(15)$  MeV in the continuum limit, are from a linear fit to data at  $\beta \geq 6.0$ . The above estimates are using  $m_s(M_K)$ . Using  $m_s(M_\phi)$  (our preferred value) would increase  $f_K$  and  $f_{D_s}$  by  $\approx 2\%$ .

We study three lattice transcriptions of the vector current to calculate  $f_V^{-1}$ . Using the Lepage-Mackenzie scheme to calculate  $Z_V$  for each of the three currents yields results that are consistent to within 10%. We extrapolate  $f_\rho^{-1}$  to the continuum limit by combining with results from the GF11 collaboration. The result is  $0.16(2)$  compared to the

experimental value of 0.199(5).

## **12. Acknowledgements**

We are very grateful to Steve Sharpe and Claude Bernard for comments on this paper, and to Chris Allton and Akira Ukawa for communicating unpublished results of the APE and JLQCD collaborations to us. These calculations have been done on the CM5 at LANL as part of the DOE HPCC Grand Challenge program, and at NCSA under a Metacenter allocation. We thank Jeff Mandula, Larry Smarr, Andy White and the entire staff at the two centers for their tremendous support throughout this project.

## References

- [1] C. Allton, “*LATTICE 95*”, To appear in Proceedings of the International Symposium on Lattice Field Theory, Melbourne, Australia, 1995, Eds. T. D. Kieu *et al.*, *Nucl. Phys. B (Proc. Suppl.)* , (1996), hep-lat/9509084.
- [2] T. Bhattacharya and R. Gupta, “*LATTICE 94*”, Proceedings of the International Symposium on Lattice Field Theory, Bielefeld, Germany, 1994, Eds. F. Karsch *et al.*, *Nucl. Phys. B (Proc. Suppl.)* **42**, (1995) 935.
- [3] T. Bhattacharya, R. Gupta, G. Kilcup, and S. Sharpe, LAUR-95-2354.
- [4] GF11 Collaboration, *Nucl. Phys. B***421** (1994) 217.
- [5] S. Hashimoto, “*LATTICE 95*”, To appear in Proceedings of the International Symposium on Lattice Field Theory, Melbourne, Australia, 1995, Eds. T. D. Kieu *et al.*, *Nucl. Phys. B (Proc. Suppl.)* , (1996), hep-lat/9510033.
- [6] C. Allton, *et al.* , “*LATTICE 93*”, Proceedings of the International Symposium on Lattice Field Theory, Dallas, U.S.A., 1993, Eds. T. Draper *et al.*, *Nucl. Phys. B (Proc. Suppl.)* **34**, (1994) 456, and private communications.
- [7] C. Bernard *et al.* , “*LATTICE 95*”, To appear in Proceedings of the International Symposium on Lattice Field Theory, Melbourne, Australia, 1995, Eds. T. D. Kieu *et al.*, *Nucl. Phys. B (Proc. Suppl.)* , (1996), hep-lat/9509045.
- [8] H. Hamber and G. Parisi, *Phys. Rev.* **D27**, 208 (1983).
- [9] Particle Data Book, *Phys. Rev.* **D50** (1994) 1173.
- [10] C. T. H. Davies, *et al.* , NRQCD collaboration, *Phys. Rev.* **D50** (1994) 6963.
- [11] J. Donoghue, B. Holstein, D. Wyler, *Phys. Rev. Lett.* **69** (1992) 3444.
- [12] S. Sharpe, *Phys. Rev.* **D41** (1990) 3233, *Phys. Rev.* **D46** (1992) 3146 ;  
J. Labrenz, S. Sharpe, “*LATTICE 93*”, Proceedings of the International Symposium on Lattice Field Theory, Dallas, U.S.A., 1993, Eds. T. Draper *et al.*, *Nucl. Phys. B (Proc. Suppl.)* **34**, (1994) , 335 ;  
S. Sharpe, 1994 TASI lectures, hep-ph/9412243
- [13] C. Bernard and M. Golterman, *Phys. Rev.* **D46** (1992) 853 ;  
M. Golterman, hep-lat/9405002 and hep-lat/9411005.
- [14] S. Sharpe, private communications.
- [15] R. Gupta, *Nucl. Phys. B (Proc. Suppl.)* **42** (1995) 85.
- [16] C. Bernard, “*LATTICE 93*”, Proceedings of the International Symposium on Lattice Field Theory, Dallas, U.S.A., 1993, Eds. T. Draper *et al.*, *Nucl. Phys. B (Proc. Suppl.)* **34**, (1994) 47.